

AD-A062 886

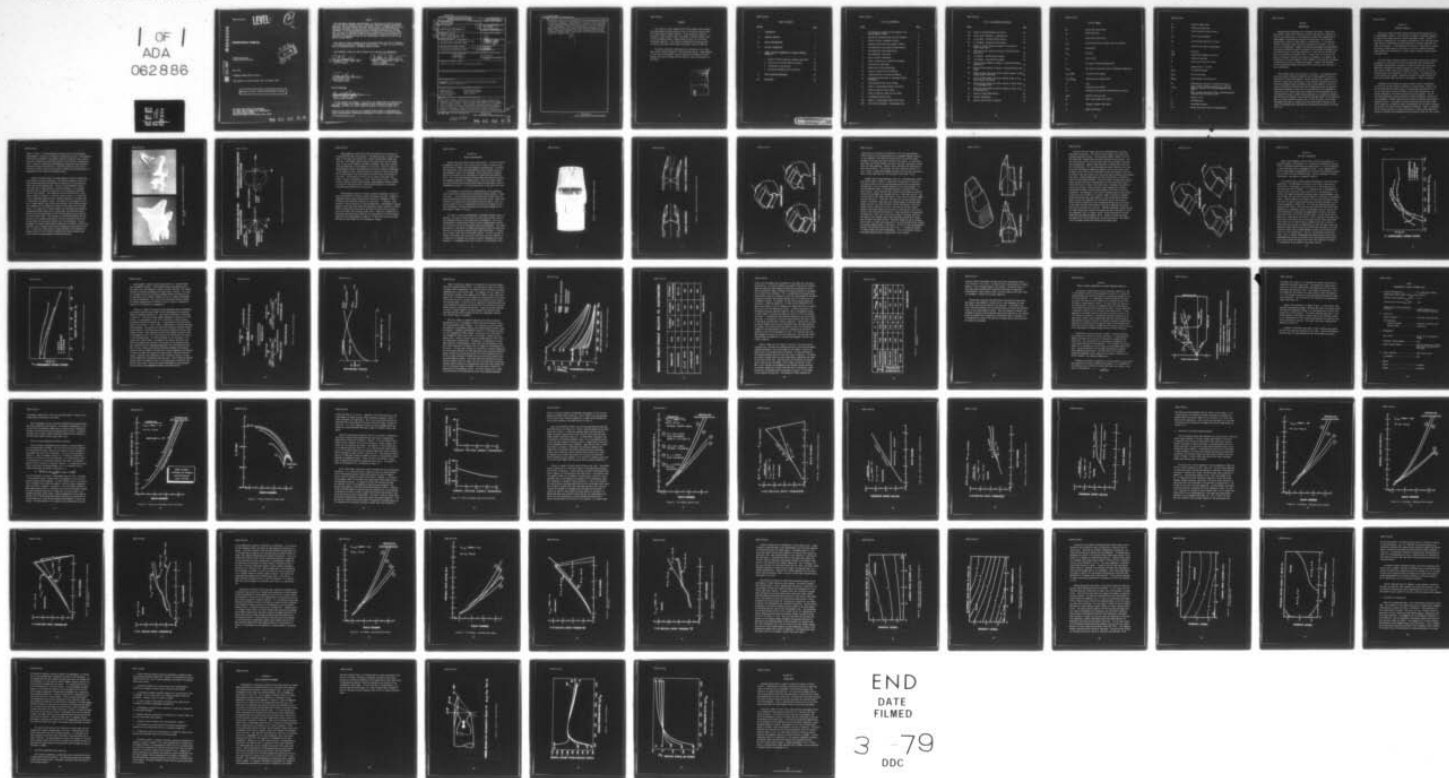
AIR FORCE AERO PROPULSION LAB WRIGHT-PATTERSON AFB OHIO
ADVANCED NOZZLE TECHNOLOGY.(U)
JUN 78 L D WOLFE, A E FANNING
AFAPL-TR-78-20

F/G 21/5

UNCLASSIFIED

NL

1 OF 1
ADA
062886



END
DATE
FILMED

3 -79
DDC

AFAPL-TR-78-20

LEVEL *II*

(2)
5

AD A062886

ADVANCED NOZZLE TECHNOLOGY

Performance Branch
Turbine Engine Division

DDC
RECEIVED
JAN 4 1979
RESISTED
F

June 1978

TECHNICAL REPORT AFAPL-TR-78-20

Final Report for Period January 1977 to January 1978

Approved for public release; distribution unlimited .

AIR FORCE AERO PROPULSION LABORATORY
AIR FORCE WRIGHT AERONAUTICAL LABORATORIES
AIR FORCE SYSTEMS COMMAND
WRIGHT-PATTERSON AIR FORCE BASE, OHIO 45433

79 01 02 010

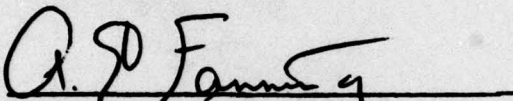
DDC FILE COPY

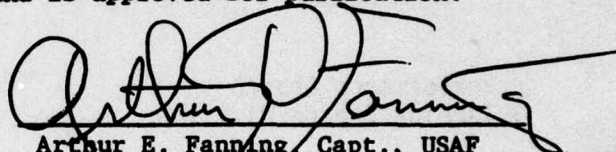
NOTICE

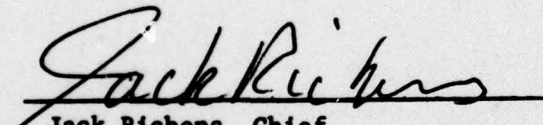
When Government drawings, specifications, or other data are used for any purpose other than in connection with a definitely related Government procurement operation, the United States Government thereby incurs no responsibility nor any obligation whatsoever; and the fact that the government may have formulated, furnished, or in any way supplied the said drawings, specifications, or other data, is not to be regarded by implication or otherwise as in any manner licensing the holder or any other person or corporation, or conveying any rights or permission to manufacture, use, or sell any patented invention that may in any way be related thereto.

This report has been reviewed by the Information Office (OI) and is releasable to the National Technical Information Service (NTIS). At NTIS, it will be available to the general public, including foreign nations.

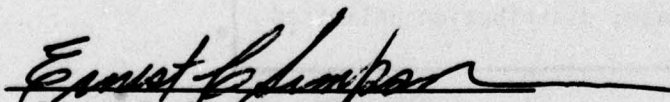
This technical report has been reviewed and is approved for publication.


for Lawrence D. Wolfe, Capt., USAF
Project Engineer


Arthur E. Fanning, Capt., USAF
Technical Manager
Turbine Engine Performance


Jack Richens, Chief
Performance Branch

FOR THE COMMANDER


Ernest C. Simpson, Director
Turbine Engine Division

"If your address has changed, if you wish to be removed from our mailing list, or if the addressee is no longer employed by your organization please notify AFAPL/TBA, W-PAFB, OH 45433 to help us maintain a current mailing list".

Copies of this report should not be returned unless return is required by security considerations, contractual obligations, or notice on a specific document.

UNCLASSIFIED

SECURITY CLASSIFICATION OF THIS PAGE (When Data Entered)

REPORT DOCUMENTATION PAGE		READ INSTRUCTIONS BEFORE COMPLETING FORM
1. REPORT NUMBER AFAPL-TR-78-20	2. GOVT ACCESSION NO.	3. RECIPIENT'S CATALOG NUMBER
4. TITLE (and Subtitle) ADVANCED NOZZLE TECHNOLOGY	5. TYPE OF REPORT & PERIOD COVERED Final Report, Jan 77 - Jan 78	6. PERFORMING ORG. REPORT NUMBER
7. AUTHOR(s) Lawrence D. Wolfe, Capt, USAF Arthur E. Fanning, Capt, USAF	8. CONTRACT OR GRANT NUMBER(s)	
9. PERFORMING ORGANIZATION NAME AND ADDRESS Air Force Aero Propulsion Laboratory (TBA) Wright-Patterson AFB, Ohio 45433	10. PROGRAM ELEMENT, PROJECT, TASK AREA & WORK UNIT NUMBERS Proj 3066 Task 11 Work Unit 08	
11. CONTROLLING OFFICE NAME AND ADDRESS Air Force Aero Propulsion Laboratory (TBA) Wright-Patterson AFB, Ohio 45433	12. REPORT DATE June 1978	
14. MONITORING AGENCY NAME & ADDRESS (if different from Controlling Office) 1276p.	13. NUMBER OF PAGES 76	
	15. SECURITY CLASS. (of this report) Unclassified	
	15a. DECLASSIFICATION/DOWNGRADING SCHEDULE	
16. DISTRIBUTION STATEMENT (of this Report) Approved for public release; distribution unlimited.		
17. DISTRIBUTION STATEMENT (of the abstract entered in Block 20, if different from Report)		
18. SUPPLEMENTARY NOTES Expansion of work presented at AGARD Multi-Panel Symposium on Fighter Aircraft Design in October 1977.		
19. KEY WORDS (Continue on reverse side if necessary and identify by block number) Fighter Aircraft Variable Area Nozzles Maneuverability Thrust Vector Control Gas Turbine Engines Thrust Reversal Exhaust Nozzles		
20. ABSTRACT (Continue on reverse side if necessary and identify by block number) This report contains a description of some of the exhaust concepts being developed as design options for use on the turbine engines which will power advanced fighter aircraft. Nozzle configurations which are not axisymmetric receive the major portion of the attention. Potential benefits of these types of nozzles are discussed and three general classes of nonaxisymmetric nozzles are described. Recent work in the areas of internal nozzle performance, cooling effectiveness, and structural integrity at minimum weight		

DD FORM 1 JAN 73 1473

EDITION OF 1 NOV 65 IS OBSOLETE

UNCLASSIFIED

SECURITY CLASSIFICATION OF THIS PAGE (When Data Entered)

011570

79 01 02 010

UNCLASSIFIED

SECURITY CLASSIFICATION OF THIS PAGE(When Data Entered)

is discussed, and is used to establish the level of installation benefits which must be achieved to make these nozzles competitive with the more conventional axisymmetric configurations. The use of thrust vectoring to obtain improved normal load factor capability in an air superiority fighter was examined. Thrust accounting problems peculiar to certain nonaxisymmetric nozzles and certain thrust vectoring schemes are discussed. The report concludes with a short discussion of the further development required before these concepts can be considered as design options of acceptable risk.

UNCLASSIFIED

SECURITY CLASSIFICATION OF THIS PAGE(When Data Entered)

FOREWORD

This technical report examines some of the exhaust nozzle concepts being developed as design options for use on the turbine engines which will power advanced fighter aircraft. It was prepared in-house by Lawrence D. Wolfe, Captain, USAF, and Arthur E. Fanning, Captain, USAF, of the Performance Branch, Turbine Engine Division, Air Force Aero Propulsion Laboratory. This work was accomplished from January 1977 to January 1978 under Project 3066, Task 306611, Work Unit 30661108.

The authors gratefully acknowledge the contributions of Mr. Mark Reitz and Mr. Ronald Glidewell of the Performance Branch. Acknowledgment is also given to the General Electric Company, the McDonnell Aircraft Company, and Pratt & Whitney Aircraft Group for their contributions to the report.

ACCESSION for	
110	White Section <input checked="" type="checkbox"/>
100	Buff Section <input type="checkbox"/>
UNCLASSIFIED	<input type="checkbox"/>
CLASSIFICATION	
BY	
DISTRIBUTION/AVAILABILITY CODES	
SPECIAL	
A	

TABLE OF CONTENTS

SECTION		PAGE
I	INTRODUCTION	1
II	POTENTIAL BENEFITS	2
III	NOZZLE CONFIGURATIONS	7
IV	CRITICAL TECHNOLOGIES	15
V	THRUST VECTORING ENHANCEMENT OF AIRCRAFT MANEUVER CAPABILITY	27
	1. Effect of Thrust Vectoring on Normal Load Factor	31
	2. Sensitivity to Aircraft Design Variables	42
	3. Limitations of the Analysis	58
	4. Conclusions Regarding Thrust Vectoring	59
VI	FORCE ACCOUNTING PROCEDURES	61
VII	CONCLUSIONS	66

LIST OF ILLUSTRATIONS

FIGURE		PAGE
1	Air Superiority Fighter With Axisymmetric and Nonaxisymmetric Nozzles	4
2	Reduced and Directionalized Infrared Signature	5
3	State-of-the-Art Axisymmetric Nozzle	8
4	Reversing and Vectoring Axisymmetric Nozzle	9
5	Two-Dimensional, Convergent-Divergent Nozzle	10
6	Two-Dimensional Single Ramp Nozzle	12
7	Two-Dimensional Plug Nozzle	14
8	Nozzle Internal Performance	16
9	Effect of Vectoring on Internal Performance	17
10	Nozzle Cooling Techniques	19
11	Comparison of Cooling Techniques	20
12	Effect of Nozzle Cooling Techniques	22
13	Integrated Effect on Engine Performance	23
14	Individual Contributions to Integrated Engine Performance	25
15	Velocity-Normal Load Factor Diagram	28
16	Effect on Instantaneous Normal Load Factor	32
17	Effect on Specific Excess Power	33
18	Effect on Maneuver Speed and Turn Radius	35
19	V-N Diagram, Baseline Case	37
20a	Change in Instantaneous Normal Load Factor	38
20b	Thrust Vector Schedule - Instantaneous Turn	39

LIST OF ILLUSTRATIONS (CONTINUED)

FIGURE		PAGE
21a	Change in Sustained Normal Load Factor	40
21b	Thrust Vector Schedules - Sustained Turn	41
22	V-N Diagram - Increased Thrust Loading	43
23	V-N Diagram - Decreased Thrust Loading	44
24	Effect of Thrust Loading on Change in Instantaneous Normal Load Factor	45
25	Effect of Thrust Loading on Change in Sustained Normal Load Factor	46
26	V-N Diagram - Decreased Wing Loading	48
27	V-N Diagram - Increased Wing Loading	49
28	Effect of Wing Loading on Change in Instantaneous Normal Load Factor	50
29	Effect of Wing Loading on Change in Sustained Normal Load Factor	51
30	Effect of Wing Loading and Thrust Loading Change in Instantaneous Normal Load Factor	53
31	Effect of Wing Loading and Thrust Loading Change in Sustained Normal Load Factor	54
32	Effect of Wing Loading and Thrust Loading on Vector Angle in Instantaneous Turn	56
33	Effect of Wing Loading and Thrust Loading on Vector Angle in Sustained Turn	57
34	Family of Single Ramp Nozzles	63
35	Internal Performance	64
36	Angle at Which Thrust Is Applied	65

LIST OF SYMBOLS

AR	Nozzle Duct Aspect Ratio
A_g	Nozzle Exit Area
C_v	Gross Thrust Coefficient
$D_{a/c}$	Drag-Aircraft Wing, Fuselage, and Tail Surfaces
D_{can}	Drag-Canard
D_{ram}	Drag-Ram
F_g	Gross Thrust
F_n	Net Thrust at Maximum Augmentation
$F_{n_{sls}}$	Net Thrust at Sea Level Static and Maximum Augmentation
$F_{n_{sls}}/TOGW$	Aircraft Thrust Loading
$F_{n_{sls}}/Wgt_{eng}$	Engine Thrust to Weight Ratio
FT	Feet
g	Constant 32.174 ft/sec ²
G's	Acceleration Normalized by Acceleration of Gravity
Knots	Nautical Miles per hour
\dot{M}_g	Mass Flow at Nozzle Exit Plane
ΔN	Changes in Normal Load Factor
N	Normal Load Factor

P_s	Specific Excess Power
psf	Pounds per Square Foot
P_8	Total Pressure at Nozzle Throat
P_{so}	Static Pressure-Ambient
P_{s9}	Static Pressure-Nozzle Exit Plane
R	Aircraft Turn Radius-Instantaneous
S, S_w	Wing Area
TOGW	Takeoff Gross Weight of Aircraft
V	Velocity-Freestream
V_9	Velocity at Nozzle Exit Plane
W	Combat Weight of Aircraft
W_{fuel}	Fuel Weight-Internal
W_{cool}	Cooling Flow Rate
$W_{t_{eng}}$	Engine Weight Including Nozzle
X/L	Nondimensional distance in freestream direction
δ_v, δ_{ap}	Angle at Which Vectored Thrust Force is Applied, Measured Clockwise From Fuselage Reference Line (FRL).
\uparrow	Angle to Which Nozzle Exit Plane is Rotated Measured Clockwise From Line Normal to FRL
Δ	Change in Value
2-D	Two-Dimensional
C-D	Convergent-Divergent
V-N	Normal Load Factor Versus Airspeed Diagram

SECTION I

INTRODUCTION

Advanced nozzle technology is an extremely broad topic. Rather than try to give a review of all the work in each of the technical subareas related to this broad topic, in this report the authors have concentrated on nonaxisymmetric configurations and the work being done in the technical subareas most critical to these types of configurations. It is important to bear in mind that neither the areas discussed nor the depth in any one area is all encompassing. However, the advanced techniques and technologies discussed are frequently equally applicable to conventional axisymmetric nozzle configurations, so that the nonspecialist in any one area can read the work as an overview of the entire area. It seems only fair to define the point of reference from which this report was assembled. The authors view the nozzle as first and foremost a basic component of the engine, and attempt to maintain this point of reference throughout. However, the importance of the interactions between the engine with its nozzle and the airframe is fully appreciated.

The following topics are discussed in the report: The potential benefits which might be obtained through the use of nonaxisymmetric nozzles; a description of three nonaxisymmetric nozzle configurations; examples of the results of recent tests and analysis in the technical areas most critical to achieving acceptable engine performance with a nonaxisymmetric nozzle; the level of installation benefits which must be obtained to make the installed performance comparable to that which can be obtained with an axisymmetric nozzle; the use of thrust vectoring to enhance aircraft maneuverability and the importance of basic aircraft design parameters to the degree of enhancement which can be achieved; force accounting problems unique to the nonaxisymmetric or thrust vectoring nozzles; and, a brief discussion of the further development work which is required to bring these types of nozzles to the stage of development where they might be considered design options of acceptable risk.

SECTION II

POTENTIAL BENEFITS

There are a number of benefits which might be derived through the use of nonaxisymmetric nozzles. The most basic of these is improved integration of engine and airframe to obtain a better aerodynamic design. Benefits in the areas of detectability, and therefore vulnerability, also have been postulated based on directionalization and reduction of infrared signatures and radar cross sections. If the penalties for the use of these types of nozzles are offset by other benefits, then there can also be a potential reduced weight penalty for incorporation of either thrust reversal or thrust vectoring capabilities.

For the variety of reasons including twin engine reliability, improved aerodynamics at high angles of attack, and numerous other structural and aerodynamic considerations, designers of combat aircraft have nearly abandoned their predisposition toward fuselages of circular cross section. Even our most recent single engine fighter aircraft, the F16, has a fuselage which upon close inspection is far from circular. The propulsion side of the industry has, however, steadfastly refused to consider turbines of other than circular cross sections, a trend which is likely to continue.

Blending of the airframe and engine to obtain superior aerodynamics can be one of the most difficult problems of aircraft design. Much of the zero lift drag of an aircraft occurs on the afterbody and nozzle and it is in this region that care must be taken to ensure good recompression and prevent separation in the resulting adverse pressure gradient. The complex three-dimensional contours required to blend axisymmetric nozzles with non-axisymmetric airframes complicate the problem by steepening the pressure gradients locally. The problem is further complicated by the need to keep nozzle length to a minimum for weight considerations and the need to incorporate variable exit area to obtain acceptable performance. Planar or nonaxisymmetric nozzles provide an excellent opportunity to reduce three-dimensional effects by spreading the recompression more uniformly around the cross section.

Shown in Figure 1 is the aesthetically pleasing result of incorporating nonaxisymmetric nozzles on a current air superiority aircraft. Unfortunately, quantitative assessment of the benefits actually derived on such a vehicle must await completion of extensive testing of such realistic configurations. So far, extensive drag data on nonaxisymmetric nozzles has been limited to some basic research configurations. The USAF and NASA are currently conducting wind tunnel tests on more realistic fighter type configurations, and quantitative results should be available shortly.

Another potential benefit of nonaxisymmetric nozzles is reduced and directionalized infrared signatures. The infrared signature consists of the radiation emanating from both the hot metal parts of the engine and nozzle and the hot exhaust gases. The use of nonaxisymmetric nozzles can affect both of these sources of infrared radiation. The signature radiating from hot engine or nozzle parts can be reduced by providing line of sight blockage. This signature can be directionalized in cases where it cannot be reduced. On the left side of Figure 2 is a depiction of the intermediate power hot parts infrared signature of an engine with a conventional axisymmetric nozzle. By replacing the axisymmetric nozzle with a nonaxisymmetric plug nozzle which provides line-of-sight blockage, this signature can be reduced to the small ellipse depicted on the same figure. The right side of Figure 2 depicts how replacing an axisymmetric convergent-divergent nozzle with a single ramp, two-dimensional nozzle affects the directionalization of the infrared signature due to both hot parts and exhaust plume. This reduction in radiation emanating from the hot gases in the exhaust plume results from the increased mixing of the exhaust plume with the cooler external air of the freestream. The non-axisymmetric concepts provide more circumference surrounding a given cross-sectional area of exhaust plume, thus providing more surface area for mixing. In some cases, the mixing is further enhanced by the formation of strong vortices in the vicinity of sidewalls and corners caused by the locally severe pressure gradients around these corners.

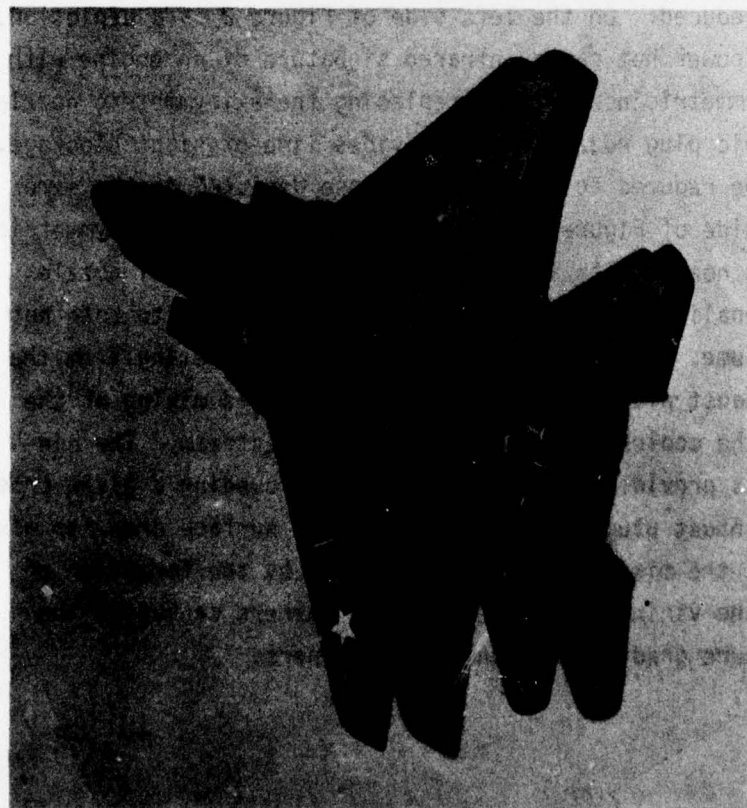
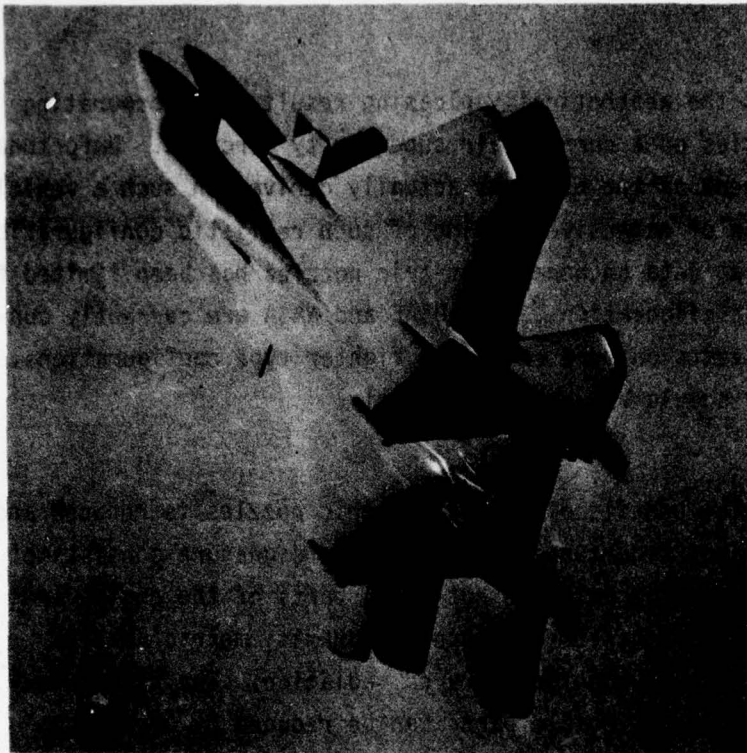


Figure 1. Air Superiority Fighter With Axisymmetric and Nonaxisymmetric Nozzles

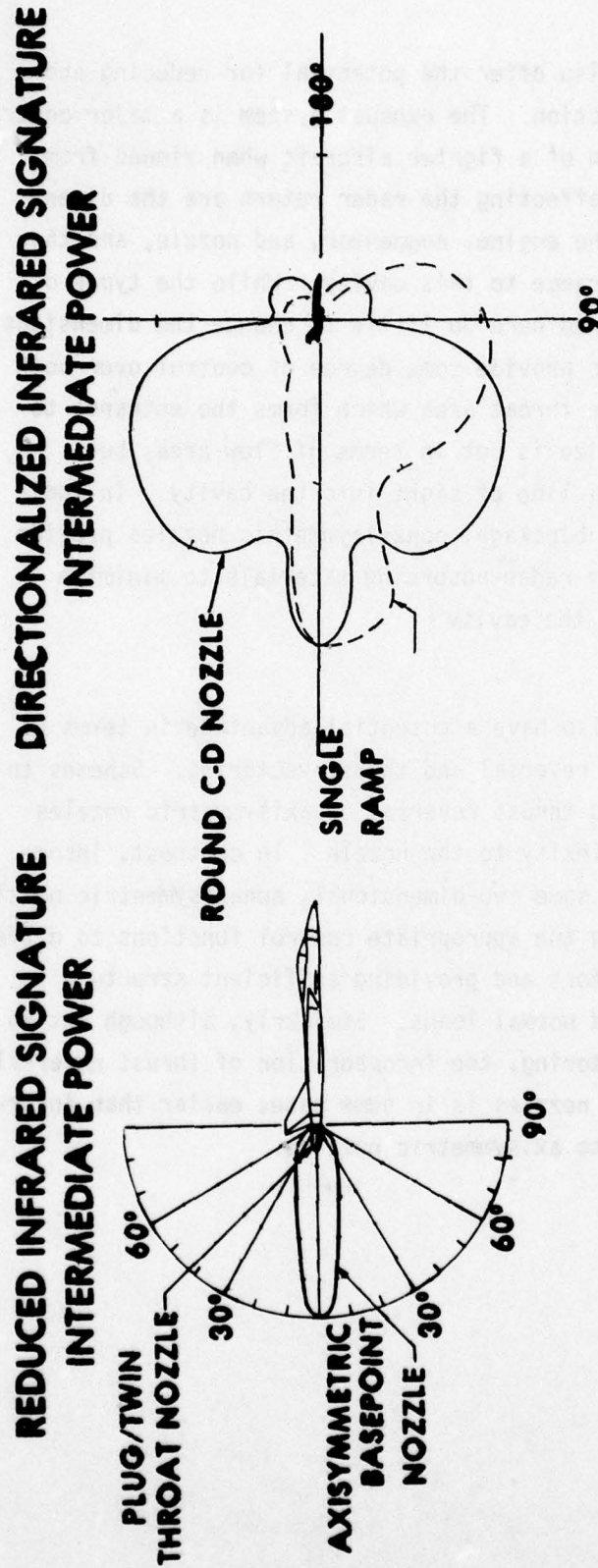


Figure 2. Reduced and Directionalized Infrared Signature

Nonaxisymmetric nozzles also offer the potential for reducing and directionalizing radar cross section. The exhaust system is a major contributor to the radar cross section of a fighter aircraft when viewed from the rear. The primary factors affecting the radar return are the dimensions of the cavity formed by the engine, augmentor, and nozzle, and the shape and dimensions of the entrance to this cavity. While the types of nonaxisymmetric nozzles considered here do little to change the dimensions of the augmentor cavity, they do provide some degree of control over both the size and shape of the nozzle throat area which forms the entrance to the cavity. The variation in size is not in terms of flow area, but rather in terms of blockage of a line of sight into the cavity. In addition to providing line-of-sight blockage, nonaxisymmetric nozzles provide a surface for the application of radar absorbing materials to minimize reflection entering and exiting the cavity.

Nonaxisymmetric nozzles also have a potential advantage in terms of ease of incorporation of thrust reversal and thrust vectoring. Schemes to incorporate thrust vectoring and thrust reversal on axisymmetric nozzles frequently add significant complexity to the nozzle. In contrast, incorporation of thrust vectoring on some two-dimensional, nonaxisymmetric nozzles requires little more than adding the appropriate control functions to differentially operate existing actuators and providing sufficient structure to carry and transmit the increased normal loads. Similarly, although not to the extent encountered with vectoring, the incorporation of thrust reversal capability into nonaxisymmetric nozzles is in some cases easier than incorporating the same capability into axisymmetric nozzles.

SECTION III

NOZZLE CONFIGURATIONS

Consider now some various nozzle configurations. A state-of-the-art axisymmetric nozzle will first be described in order to provide a base against which to compare the nonaxisymmetric configurations. Following this description, the significant features of each of three classes of nonaxisymmetric nozzles are described. All of the nozzles considered here are self-cooled by fan discharge air routed behind the augmentor liner. All of the configurations provide throat area variation suitable for augmented operation on turbofan cycles. Also, all designs feature exit area variation which may be either slaved to throat area or may be independently variable. All thrust vectoring is in the pitch plane only.

An axisymmetric nozzle which is representative of the technology level found on most advanced current production fighter engines is shown in Figure 3. It has a peak gross thrust coefficient of over 0.985, and requires approximately 8% of the engine airflow for cooling. Throat area variation is accomplished with overlapping flaps and seals. Thrust reversing capability can be incorporated by the use of a blocker and cascade arrangement, and thrust vectoring can be achieved through use of a dual gimbal as shown in Figure 4.

In Figure 5 a simple two-dimensional, convergent-divergent nozzle is depicted. The cross sections at the exit, the throat, and the inlet to the convergent portion of the nozzle are all rectangular. As with all nonaxisymmetric configurations, there is a duct upstream which provides the transition from the circular cross section of the engine. The convergent section of the nozzle is formed by two planar flaps, and throat area variation is achieved by actuators moving these two surfaces. A second pair of planar flaps forms the divergent section. The exit area may be slaved to the throat area to provide a specified area ratio schedule, or a second set of actuators can be used to provide independent exit area variation. If independent area ratio variation is incorporated, thrust

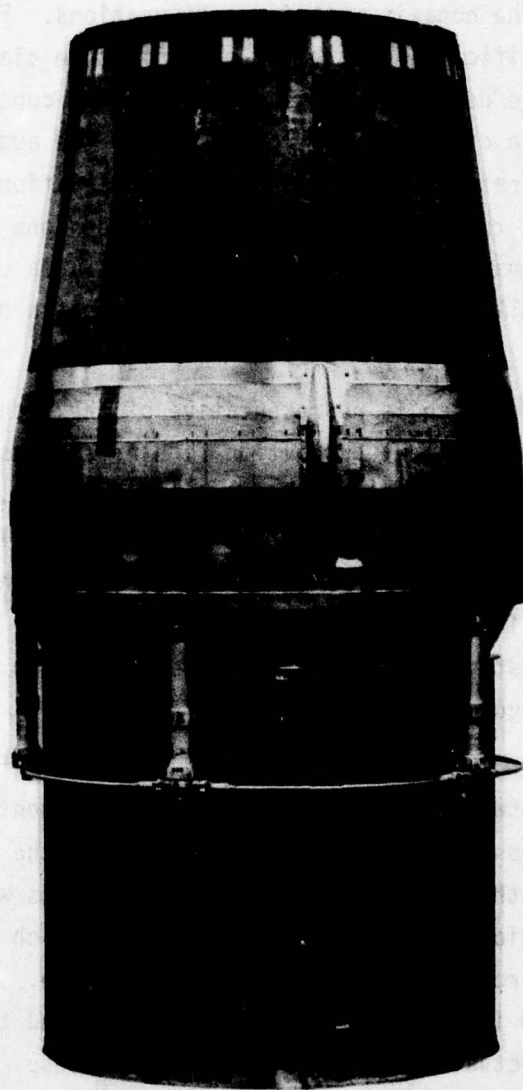
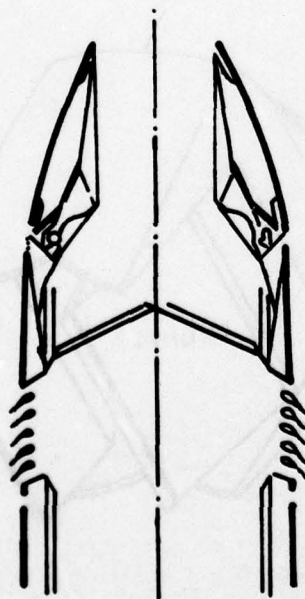
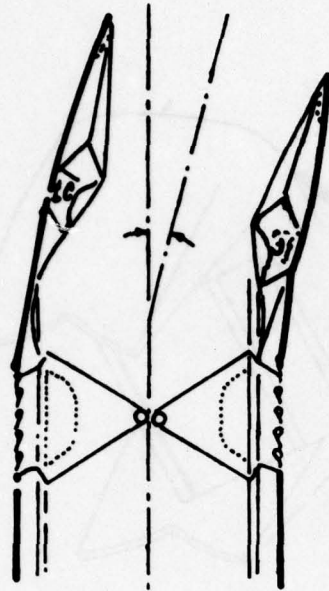


Figure 3. State-of-the-Art Axisymmetric Nozzle



THRUST REVERSING



THRUST VECTORING (GIMBAL)

Figure 4. Reversing and Vectoring Axisymmetric Nozzle

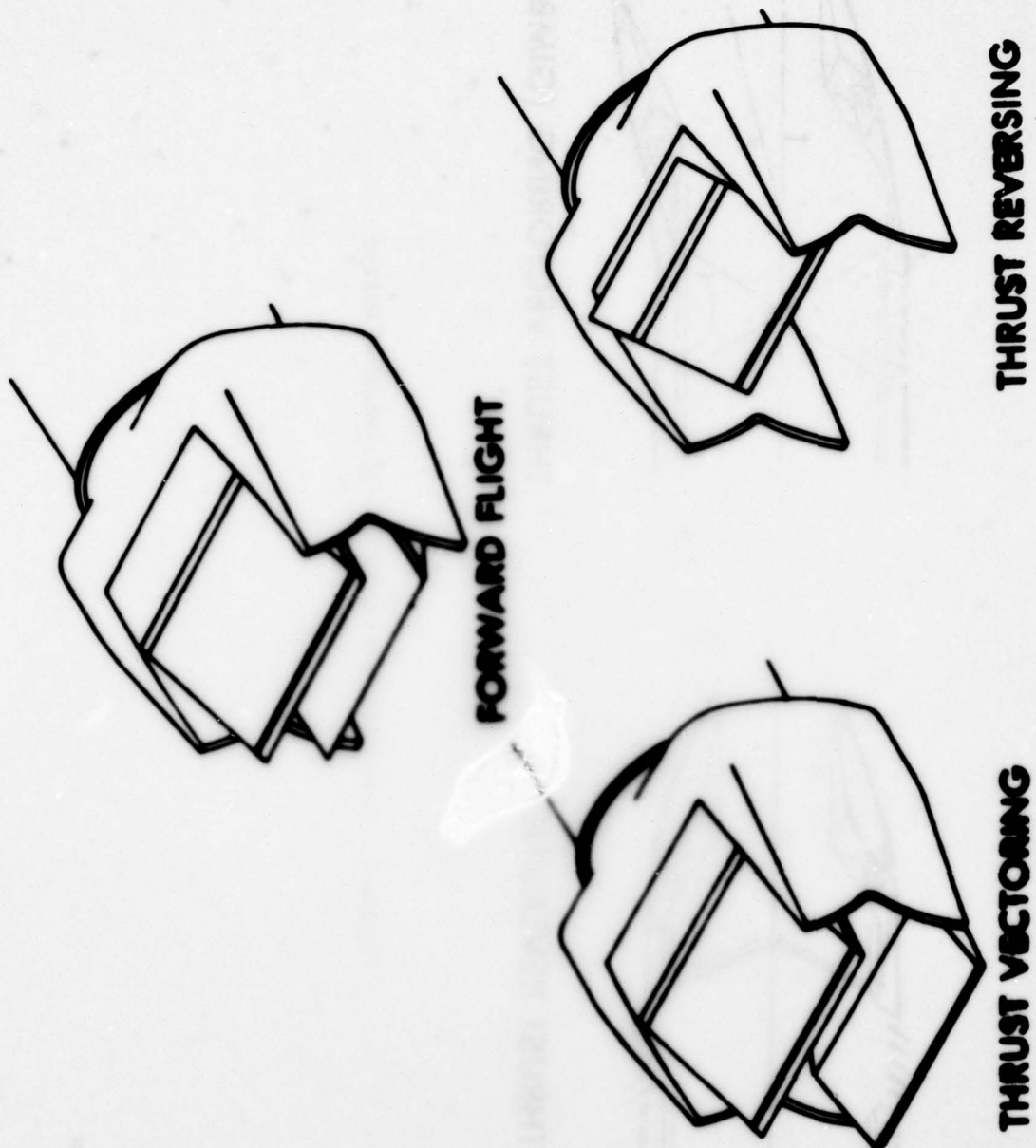
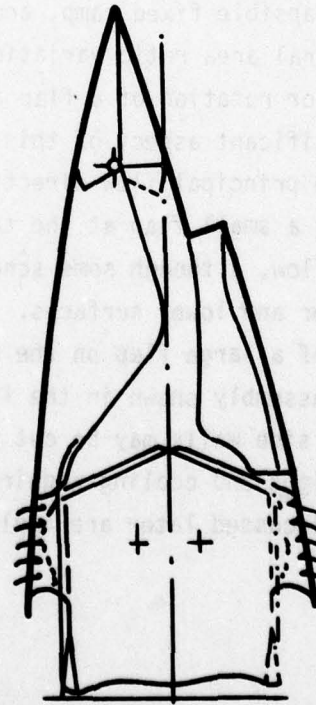
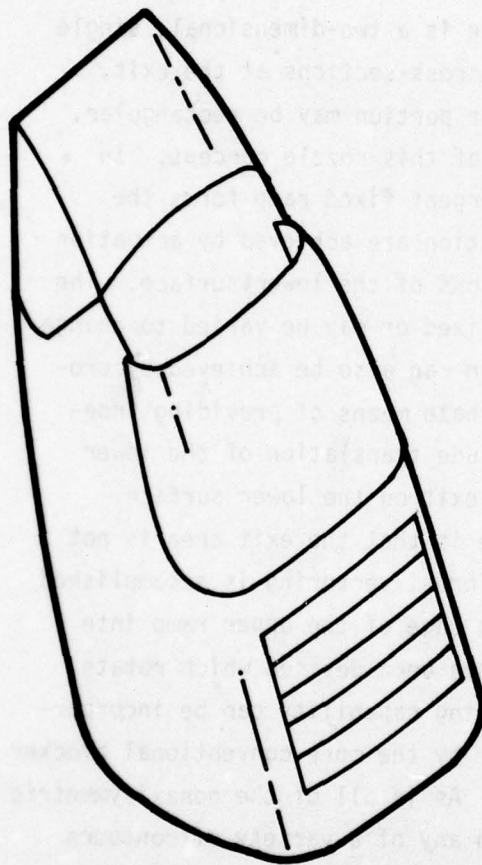


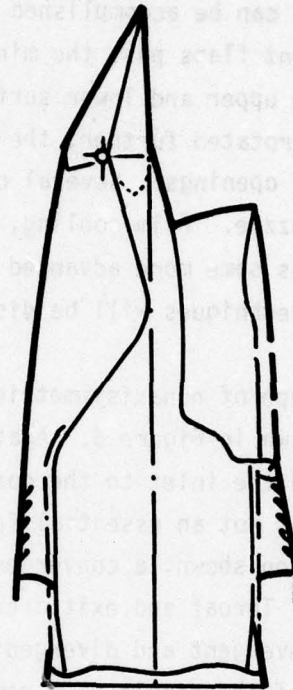
Figure 5. Two-Dimensional, Convergent-Divergent Nozzle

vectoring can be achieved by differential use of the same actuators. Thrust reversal can be accomplished by an arrangement whereby rotation of the convergent flaps past the minimum throat area position opens passages on the upper and lower surfaces of the nozzle. As the convergent flaps are rotated further, the total flow area transitions to these upper and lower openings. Several cooling techniques are applicable to this type of nozzle. Film cooling, film plus convection cooling, fin wall, as well as some more advanced techniques could be used effectively. These cooling techniques will be discussed in more detail later.

Another type of nonaxisymmetric nozzle is a two-dimensional, single ramp nozzle shown in Figure 6. Again the cross-sections at the exit, the throat, and the inlet to the convergent portion may be rectangular, although this is not an essential feature of this nozzle concept. In the configuration shown, a convergent-divergent fixed ramp forms the upper surface. Throat and exit area variation are achieved by actuation of both the convergent and divergent portions of the lower surface. The trailing edge of the single ramp remains fixed or may be varied to change internal area ratio. Throat area variation can also be achieved by providing a collapsible fixed ramp, and alternate means of providing independent internal area ratio variation include translation of the lower surface cowl or rotation of a flap at the exit on the lower surface. The most significant aspect of this nozzle is that the exit area is not normal to the principal flow direction. Thrust vectoring is accomplished by deflecting a small flap at the trailing edge of the upper ramp into the exhaust flow, although some schemes have been devised which rotate both the upper and lower surfaces. Resersing capability can be incorporated by use of a large flap on the plug or by the more conventional blocker and cascade assembly shown in the figure. As in all of the nonaxisymmetric nozzles, the side walls may be cut back in any of a variety of contours to reduce weight and cooling requirements. All of the advanced cooling techniques discussed later are applicable to this concept.



THRUST REVERSING



THRUST VECTORING

Figure 6. Two-Dimensional Single Ramp Nozzle

The third and last nozzle type to be considered here is the two-dimensional plug nozzle. This nozzle can be viewed as two single ramp nozzles placed back to back. The plug nozzle shown in Figure 7 will be described here, although there are many variations on this design. Like the single ramp nozzle, the plug nozzle tends to be altitude or pressure ratio compensating. However, some variation in internal area ratio may still be desirable. This can be achieved by either rotation of the flaps which form the boundary between the external flow and the exhaust flow as shown in the figure or by translation of these same flaps in the axial direction so that the internal area ratio more nearly approaches the external area ratio. Alternate approaches involving translating or collapsible plugs are also being considered. With the variable incidence plug configuration, thrust vectoring is accomplished by pivoting the entire plug to direct the flow up or down in the pitch plane. Divergent flap position can also be varied in conjunction with plug incidence angle and more sophisticated schemes involving adding camber to the plug can also be considered. One advantage of the variable incidence plug is that turning of the flow occurs primarily at subsonic speeds, resulting in somewhat reduced vectoring losses when compared to flap and deflection surfaces which turn the flow supersonically through the use of oblique shocks. Thrust reversal capability can be incorporated through the use of flaps on the upper and lower plug surfaces which may be deployed into the exhaust jet to block and turn the flow. Alternate approaches include the use of a more conventional blocker and cascade upstream of the plug, or using the convergent flaps in a manner similar to that described for the two-dimensional convergent-divergent nozzle. Advanced cooling techniques are required for the two-dimensional plug nozzle because of the substantially increased surface area wetted by the exhaust gases.

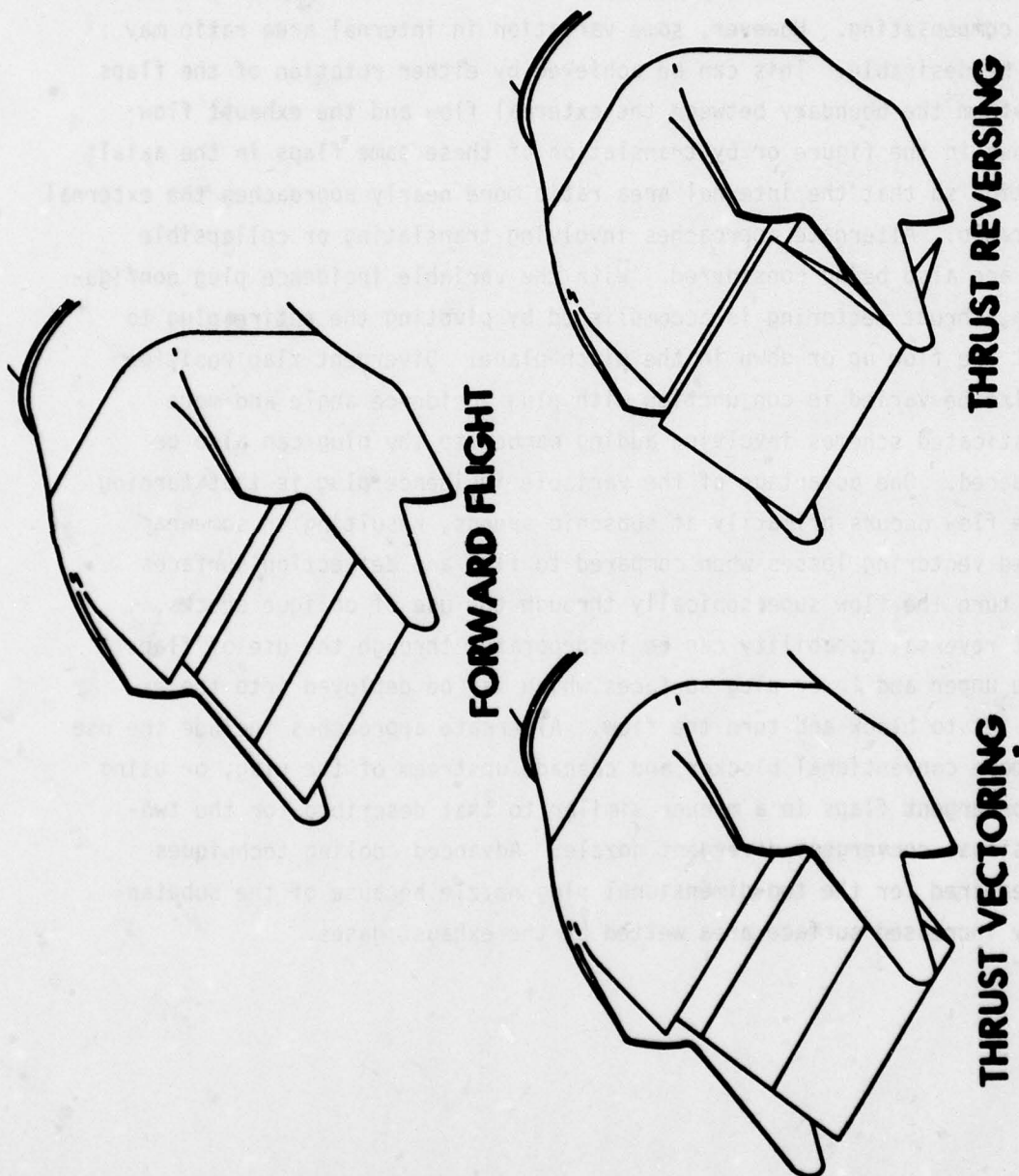


Figure 7. Two-Dimensional Plug Nozzle

SECTION IV

CRITICAL TECHNOLOGIES

Before nonaxisymmetric nozzles can be seriously considered as an option available to the designer, it is necessary to demonstrate that the level of performance achievable with these nozzles is at least comparable to that achievable with an axisymmetric concept. Such a demonstration requires development and demonstration of the level of performance achievable in certain critical technical areas: internal performance, cooling requirements, and weight or structural integrity.

The primary index of nozzle internal performance is the gross thrust coefficient. The importance of attaining high levels of gross thrust coefficient is self evident, since this acts as a direct multiplier on the total gross thrust produced. It is important for a nonaxisymmetric nozzle to have a high gross thrust coefficient at the design point. For a given flap length and maximum divergence angle, the nonaxisymmetric nozzle provides less area ratio variation capability than does an axisymmetric nozzle. Figure 8 depicts the variation of gross thrust with nozzle pressure ratio for each of these advanced nozzle concepts considered, as well as the axisymmetric configuration. This data was obtained from recent subscale static tests. Note that the peak gross thrust coefficient when compared to an axisymmetric nozzle is decreased by one half percent for the two-dimensional, convergent-divergent nozzle, 0.25% for the single ramp nozzle, and 1.25% for the 2-D plug nozzle. The off-design performance also is depicted on this figure. Thrust vectoring also affects the gross thrust coefficient, and the variation in gross thrust coefficient which results as the vector angle is changed can be seen in Figure 9. Some caution must be used in interpreting or using this data because the traditional definition of gross thrust coefficient used here is not well suited to certain types of nonaxisymmetric nozzles at off-design conditions or in the vectored mode. This will be discussed in more detail later. Also, it should be emphasized that these results are for static performance only and may be altered for the configurations where external flow can affect the exhaust flow field, thus resulting in changes in the pressure forces applied to the nozzle surfaces.

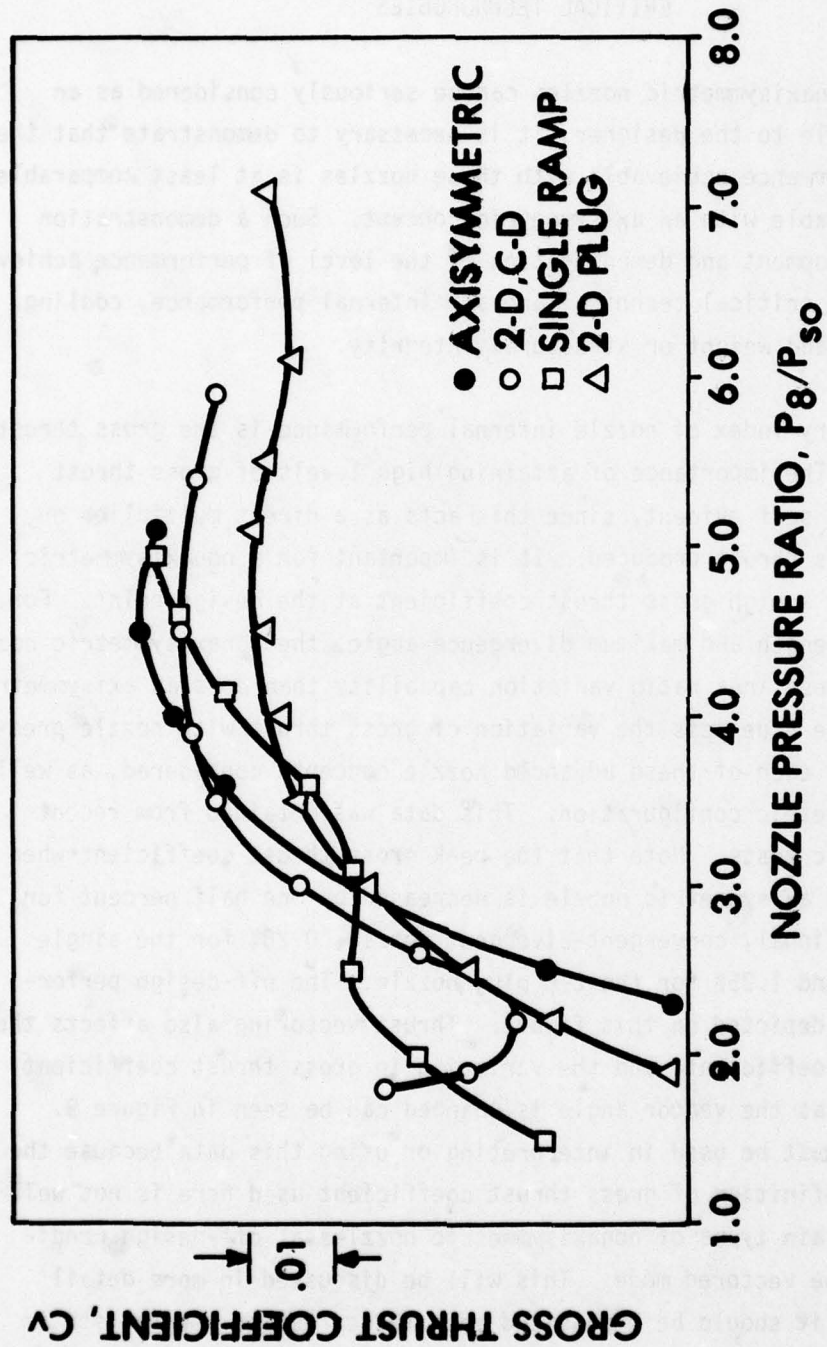


Figure 8. Nozzle Internal Performance

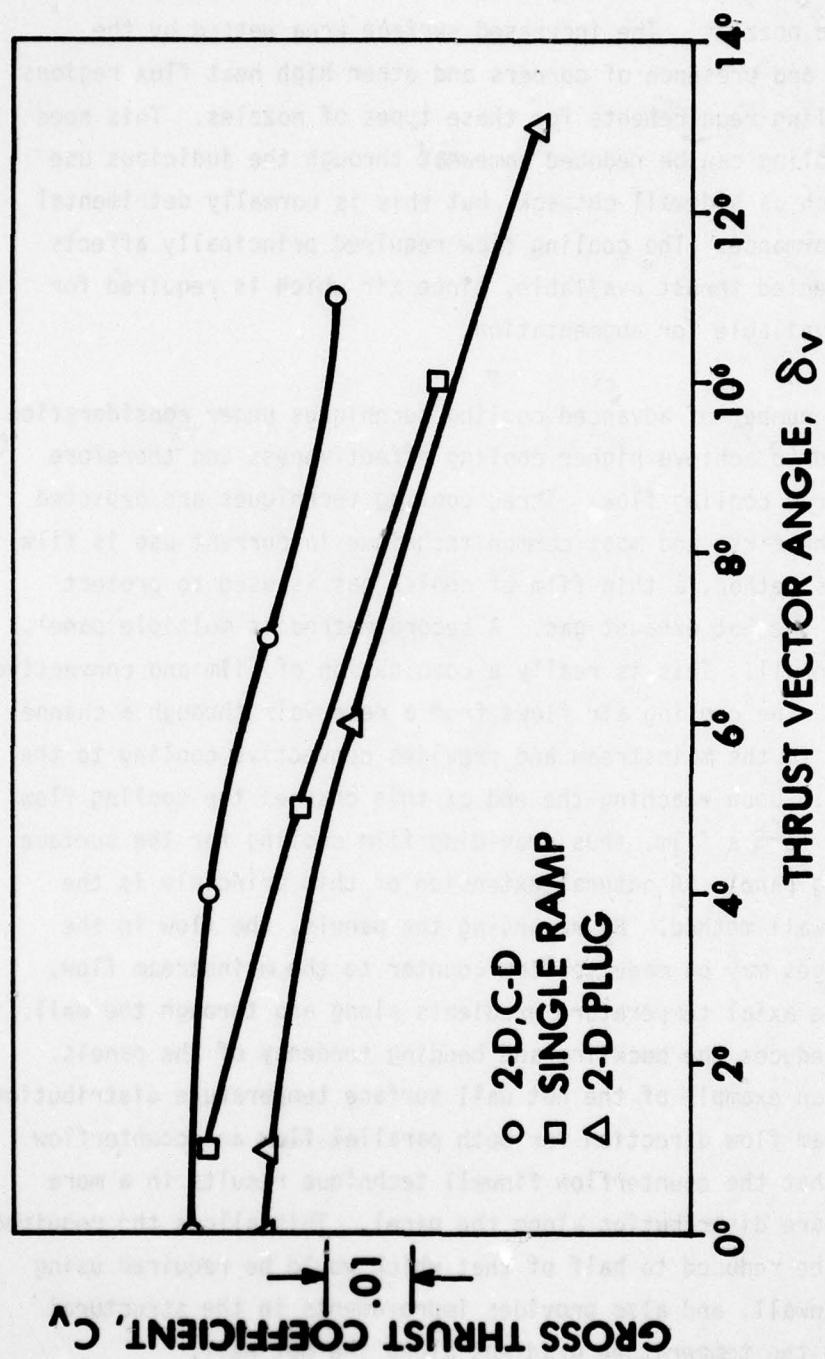


Figure 9. Effect of Vectoring on Internal Performance

Nonaxisymmetric nozzles usually present more of a cooling problem than axisymmetric nozzles. The increased surface area wetted by the hot exhaust gas, and presence of corners and other high heat flux regions increase the cooling requirements for these types of nozzles. This need for increased cooling can be reduced somewhat through the judicious use of techniques such as sidewall cutback, but this is normally detrimental to internal performance. The cooling flow required principally affects the maximum augmented thrust available, since air which is required for cooling is not available for augmentation.

There are a number of advanced cooling techniques under consideration which may be used to achieve higher cooling effectiveness and therefore reduce the required cooling flow. Three cooling techniques are depicted in Figure 10. The first and most common technique in current use is film cooling. In this method, a thin film of cooler gas is used to protect the surface from the hot exhaust gas. A second method is multiple panel, parallel flow finwall. This is really a combination of film and convective cooling methods. The cooling air flows from a reservoir through a channel running parallel to the mainstream and provides convective cooling to the channel surfaces. Upon reaching the end of this channel the cooling flow is discharged to form a film, thus providing film cooling for the surface of the succeeding panel. A natural extension of this principle is the counter flow finwall method. By reversing the panels, the flow in the convective passages may be made to flow counter to the mainstream flow, thus reducing the axial temperature gradients along and through the wall. This, in turn, reduces the buckling and bending tendency of the panels. Figure 11 shows an example of the hot wall surface temperature distribution in the main stream flow direction for both parallel flow and counterflow finwall. Note that the counterflow finwall technique results in a more uniform temperature distribution along the panel. This allows the required cooling flow to be reduced to half of that which would be required using parallel flow finwall, and also provides improvements in the structural area by reducing the temperature gradient along the hot wall.

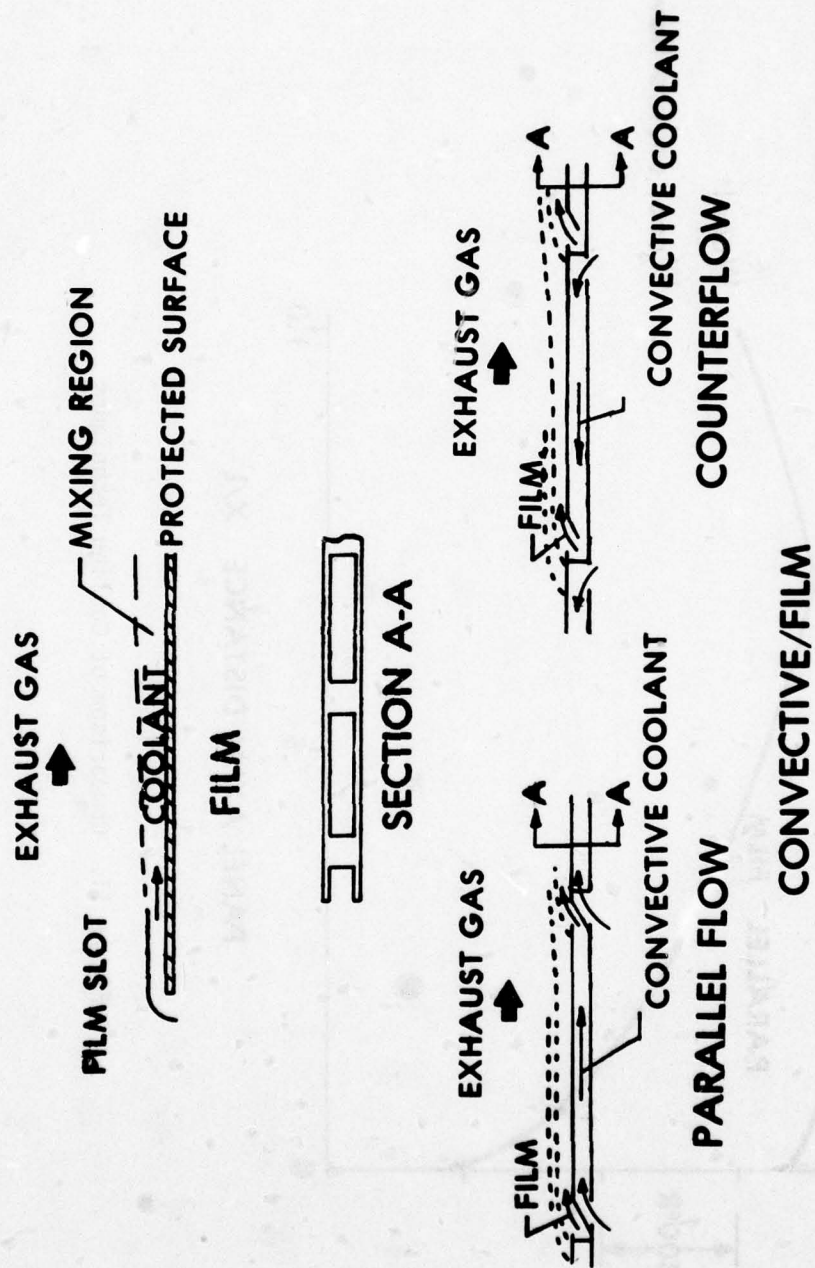


Figure 10. Nozzle Cooling Techniques

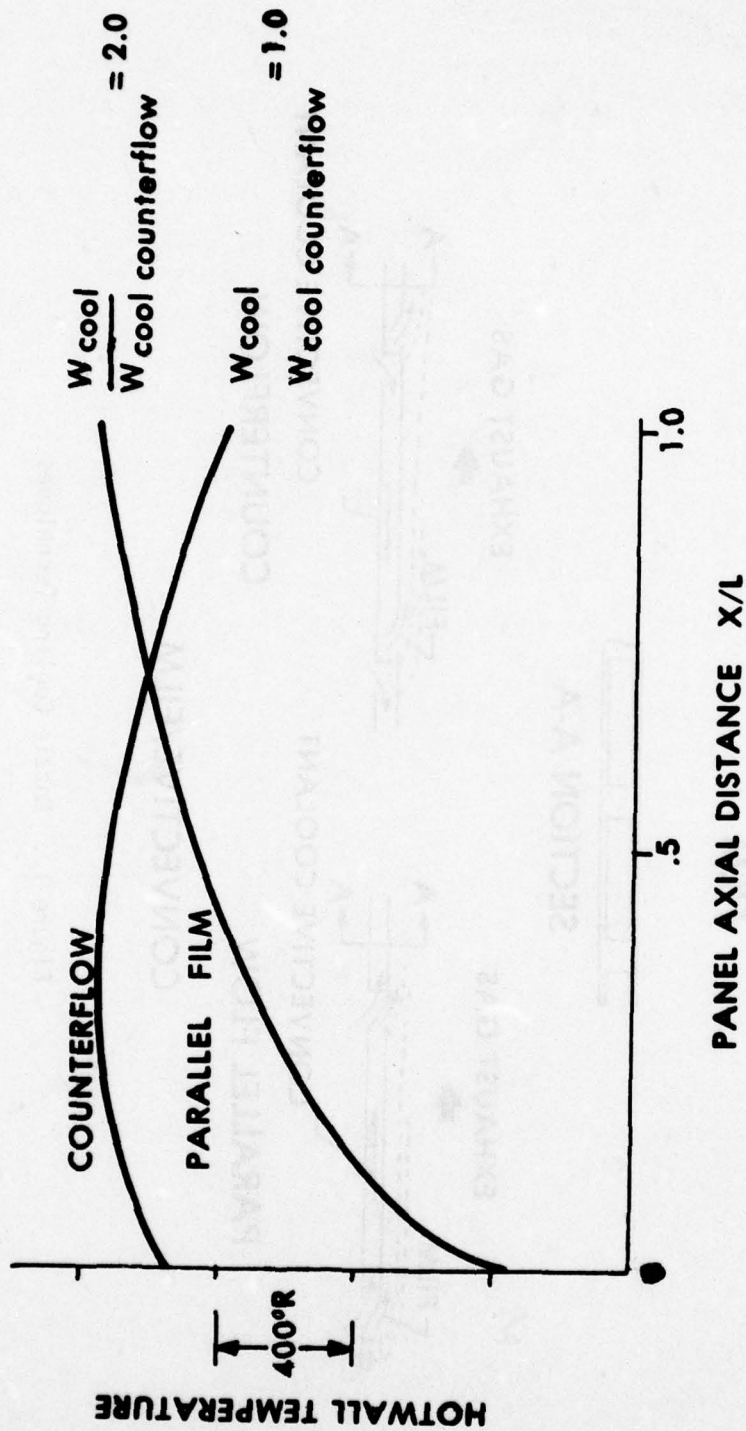


Figure 11. Comparison of Cooling Techniques

Figure 12 provides a summary of the benefits to be gained through the use of advanced cooling flows. By entering the figure at a maximum allowable surface temperature, the required specific cooling flow may be determined for a given cooling type. For example, for full length film cooling and a maximum surface temperature of 1400°F, 0.35% of the total engine flow is required for each square foot of wetted area in the nozzle. The cooling flow can be reduced to 25% of this value by using a counter flow cooling scheme. Also note that a reduction in required cooling flow can be achieved by injecting the cooling flow film at multiple locations rather than at a single upstream location. These results are expressed in terms of "panel length" or distance between film injection slots. The trend that increased allowable maximum wall temperature requires less cooling flow as is expected.

Thus far a number of potential benefits which might be derived through the use of nonaxisymmetric nozzles have been considered, along with some potential nozzle designs. It is appropriate now to consider the penalties in performance against which these potential benefits must be balanced. Although nonaxisymmetric nozzles will influence the specific fuel consumption through changes in the gross thrust coefficient, a more fundamental effect can be seen in the change in engine thrust to weight ratio. Figure 13 displays thrust to weight data for four different engine-nozzle combinations: axisymmetric; two-dimensional, convergent-divergent; two-dimensional, single ramp; and two-dimensional plug. Each column represents a different level of capability incorporated into the nozzle. The base level provides no reversing or vectoring capability. The next column represents the same type nozzle with reversing capability added, followed by the same type nozzle with vectoring capability only. The last column represents the same type nozzle with both vectoring and reversing capability added. The values shown were determined by calculating the engine thrust to weight ratio of an afterburning, mixed-flow, turbofan engine fitted with the appropriate nozzle and then dividing this value by the engine thrust to weight of the same engine fitted with a state-of-the-art axisymmetric nozzle. The thrust values used in these calculations were the uninstalled sea level static maximum augmented

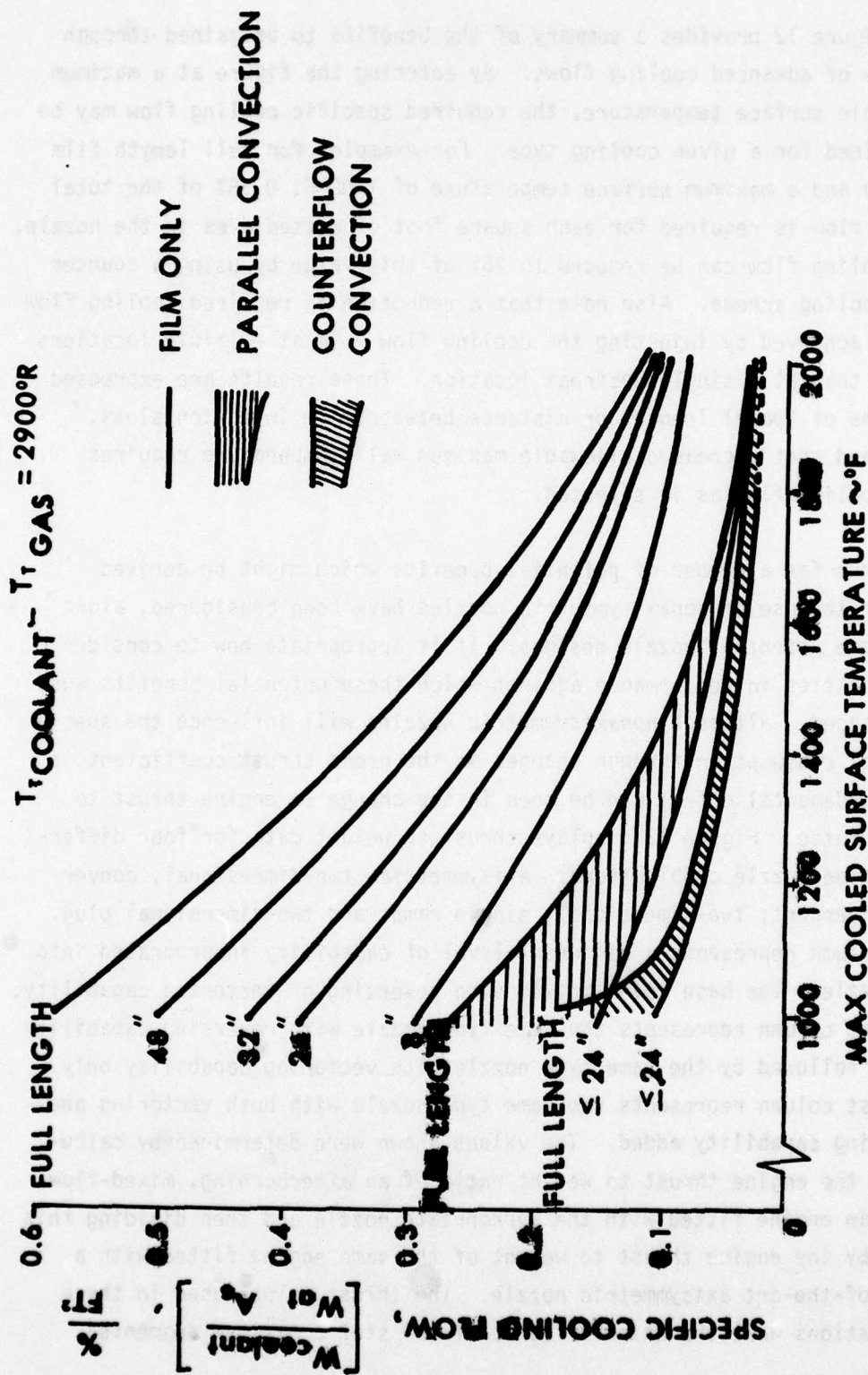


Figure 12. Effect of Nozzle Cooling Techniques

ENGINE THRUST/WEIGHT RELATIVE TO AXISYMMETRIC

NOZZLE TYPE	BASE	REVERSING ONLY	VECTORIZING ONLY	VECTORIZING AND REVERSING
AXISYMMETRIC	1.000	.911-.943	.967-.974	.893-.914
2-D, C-D AR=1.55	.961	.947	.944	.939
2-D SINGLE RAMP	.981	.934	.967	.921
2-D PLUG	.952	.911	.926	.896

SEA LEVEL STATIC

Figure 13. Integrated Effect on Engine Performance

thrusts and the weights were the weights of the engine plus the appropriate nozzle. An initial estimate can be made of the size of the drag reduction resulting from improved installation characteristics which must be achieved in order to maintain the thrust to weight of the engine at any given flight condition. This is accomplished by considering the drag reduction to be an increase in thrust and then determining the amount necessary to maintain the thrust-to-weight ratio of an engine with an axisymmetric nozzle. For example, for the 2-D C-D nozzle without any vectoring or reversing capability, in order to gain performance (i.e., thrust minus drag), it will be necessary to reduce the drag by an amount more than 3.9% of the maximum net thrust. To offset the penalty for incorporating thrust reversing capability into an axisymmetric nozzle, it would require a minimum drag reduction equal to 5.7% of the maximum net thrust. To examine the drag reduction required at any given flight condition, it is necessary to multiply these values by the thrust lapse of the engine and then make a similar comparison. These values can also be used to compare various nozzle types which have the same capability. For example, with thrust reversing capability only, the uninstalled performance of the nonaxisymmetric nozzle is competitive to marginally superior to that of the axisymmetric nozzle. For vectoring only, the nonaxisymmetric nozzles are less than competitive, and when both vectoring and reversing capability is required nonaxisymmetric nozzles are slightly superior.

Figure 14 takes the last column of Figure 13, the vectoring and reversing case, and shows the contributions made by cooling requirements, internal performance, and nozzle weight to the changes in thrust-to-weight ratio of the engines being considered. All data presented is for maximum augmented thrust at sea level static conditions. The thrust and thrust-to-weight ratio for each engine-nozzle combination was based on the same airflow size. Note that while the vectoring and reversal case is the only one considered in this figure, the top row of the matrix still depicts the axisymmetric case (without either vectoring or reversal capability) to which the other data is referenced. Note that the use of advanced cooling techniques can result in a decrease in the required cooling flow. This beneficial effect coupled with

NOZZLE TYPE	COOLING FLOW	Cv	Fn _{eds}	Wg ^t _{eng}	Fn _{alg} /Wg ^t _{eng}
W/O					
AXISYMMETRIC	1.000	1.000	1.000	1.000	1.000
W/VECTORING AND REVERSAL					
AXISYMMETRIC	1.000	1.000	1.000	1.09-1.12	.893-.914
2D-CD, AR=1.55	.385	1.013	1.025	1.09	.939
2D SINGLE RAMP	1.000	1.006	1.006	1.09	.921
2D PLUG	.50	1.026	1.037	1.16	.896

SEA LEVEL STATIC

Figure 14. Individual Contributions to Integrated Engine Performance

improved internal performance (at sea level static conditions) results in an increase in net thrust. The major driver on engine thrust to weight, however, is the increased weight of the nozzles. The overall result is that when thrust vectoring and reversing capabilities are required, a nonaxisymmetric nozzle weighs slightly less and produces more thrust than an axisymmetric nozzle with the same capability.

The previous discussion has shown that on the basis of uninstalled performance, nonaxisymmetric nozzles offer a clear advantage only when both thrust vectoring and reversing are required. In the other cases, some installation benefits must be obtained merely to offset the increased weight of the nonaxisymmetric nozzle. Since the question of whether non-axisymmetric designs provide benefits when thrust vectoring is not required cannot be answered until quantitative installation data is available, it is appropriate to consider the question of whether thrust vectoring offers any potential advantages.

SECTION V

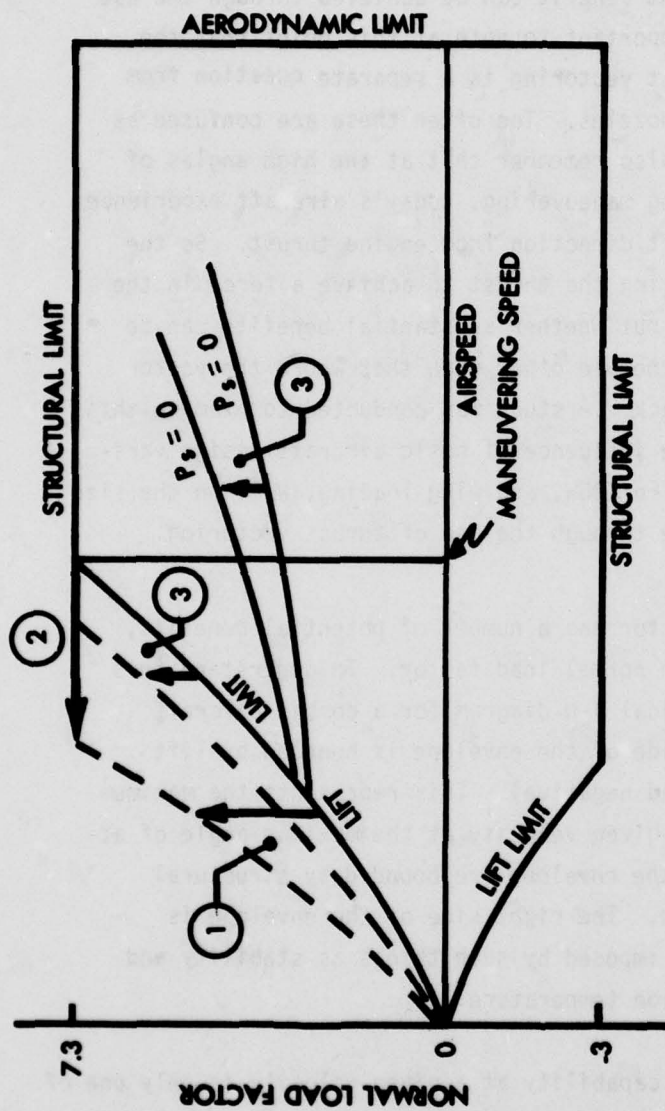
THRUST VECTORING ENHANCEMENT OF AIRCRAFT MANEUVER CAPABILITY

Since ease of incorporation of thrust vectoring capability is one of the potential benefits of nonaxisymmetric nozzles, it is logical to examine whether any significant benefit can be achieved through the use of thrust vectoring. It is important to note at this point that the question of the value of thrust vectoring is a separate question from the value of nonaxisymmetric nozzles. Too often these are confused as the same question. One must also remember that at the high angles of attack often encountered during maneuvering, today's aircraft experience a substantial force in the lift direction from engine thrust. So the question is not whether vectoring the thrust to achieve a force in the lift direction is beneficial, but whether substantial benefits can be obtained by a thrust vector schedule other than that where the vector angle equals the angle of attack. A study was conducted to examine this question, and to determine the influence of basic aircraft design variables such as thrust loading, $F_n/TOGW$, and wing loading, W/S , on the size of the improvements achievable through the use of thrust vectoring.

The ability to thrust vector has a number of potential benefits, one of which is an increase in normal load factor. To understand this benefit, consider first a typical V-N diagram for a combat aircraft (Figure 15). The left-hand side of the envelope is bounded by lift limit curves (both positive and negative). This represents the maximum number of G's achievable at a given velocity at the maximum angle of attack. The top and bottom of the envelope are bounded by structural limits imposed by the airframe. The right side of the envelope is bounded by aerodynamic limits imposed by such things as stability and control problems, and stagnation temperature.

Although an aircraft's G capability at a given velocity is only one of many capabilities relating to combat effectiveness, it is, nonetheless, a very important one. Velocity and normal load factor are related to turn radius by the equation:

$$R = \frac{v^2}{g(N^2 - 1)^{1/2}}$$



PAYOFFS EXAMINED:

- 1 INCREASE IN MAXIMUM NORMAL LOAD FACTOR (INSTANTANEOUS)
- 2 DECREASE IN MANEUVERING SPEED
- 3 NORMAL LOAD FACTOR INCREASE (INSTANTANEOUS AND SUSTAINED) WITHOUT A CORRESPONDING P_s PENALTY

Figure 15. Velocity-Normal Load Factor Diagram

To minimize turn radius, it is desirable to minimize velocity while maximizing the normal load factor. The minimum turn radius usually occurs at a velocity slightly below that where the lift limit curve intersects the structural limit. For purposes of discussion, it will be assumed that the minimum turn radius occurs at that intersection (i.e., the minimum velocity at which the maximum allowable load factor can be obtained). This velocity will be referred to as "maneuvering speed" (see Figure 15).

Payoff can be obtained in a number of ways. It could result from lowering the maneuvering speed, increasing the normal load factor obtainable below the maneuvering speed, or by decreasing the P_s penalty associated with a given maneuver. This effort explored these areas. A detailed analysis of the payoff in these areas was not intended; rather, a first approximation of the increase in maneuverability resulting from thrust vectoring was desired. The payoffs which were considered are depicted in Figure 15.

A number of assumptions were made in order to define the problem and limit the scope and complexity of the study. Careful consideration should be given to these assumptions when interpreting the results.

TABLE 1

ASSUMPTIONS OF THRUST VECTORING STUDY

1. Aircraft Configuration - - - - - air superiority fighter
Combat Wing Loading ($TOGW - 0.5W_{fuel}$)/ S_w - - - 55 lbs/ft²
Aircraft Thrust Loading $F_{n_{SLS}}/TOGW$ - - - -1.16
Internal Fuel Fraction $W_{fuel}/TOGW$ - - - -0.30

Canard (only on thrust vectoring aircraft) - - - - - located forward of c.g.,
20% of baseline wing area
2. Pitch Trim
without vectoring - - - - - horizontal stabilizer only
with vectoring
 wing and fuselage - - - - - horizontal stabilizer only
 vectored thrust - - - - - canard only
3. Aerodynamics

Basic Polar - - - - - typical of air superiority fighter
Vectoring induced changes - - - - - none
Canard induced changes - - - - - add lift and drag of isolated canard-body (no interaction with wing)
4. Thrust Vectoring - - - - - vector gross thrust
 C_v decrement - - - - - none
5. Weight
Nozzle - - - - - no penalty
Canard - - - - - no penalty

The maneuver studied was a level turn at maximum power at 30,000 ft and combat weight, 50% internal fuel weight.

Both instantaneous normal load factor capability and maximum normal load factor capability were examined. The maximum instantaneous G limit was defined by the maximum trimmed angle of attack since no maximum was reached in the lift curve below 40 degrees angle of attack. No dynamic overshoot was included. Maximum sustained G capability was defined as the point where specific excess power equals zero.

1. Effect of Thrust Vectoring on Normal Load Factor

The first payoff considered was the increase in maximum number of G's at maximum angle of attack. The lift limit curve was first defined for the baseline aircraft. Next, various amounts of thrust vectoring were added (from 15 to 60° of vectoring). The results are depicted in Figure 16. Since the number of normal G's is directly proportional to the sum of the forces in the lift direction, it is logical that if one is interested only in maximizing the normal load factor, the maximum amount of thrust vectoring is desired. However, it is important to note that in most cases, the maximum number of G's is attainable only by greatly penalizing the specific excess power, P_s .

$$P_s = \frac{[Fg \cos(\alpha + \delta_v) - (D_{ram} + D_{a/c} + D_{can})]V}{\text{Weight}}$$

and is also equal to aircraft's instantaneous rate of climb. In Figure 17, the values of specific excess power corresponding to the lift limit curves in Figure 16 are depicted. (In both Figures 16 and 17, each curve has a left-hand limit, which corresponds to the point where the maximum angle of attack is reached on the canard. Since any further decrease in Mach number would result in a situation where the pitching moment induced by thrust vectoring could not be trimmed out, the only recourse is to decrease the thrust vector angle.) Note the magnitude of the P_s penalty. At Mach 0.75, P_s ranges from approximately -850 feet per second with no thrust vectoring to -1800 feet per second with 60 degrees of thrust vectoring. This would result in an increase in the deceleration along the

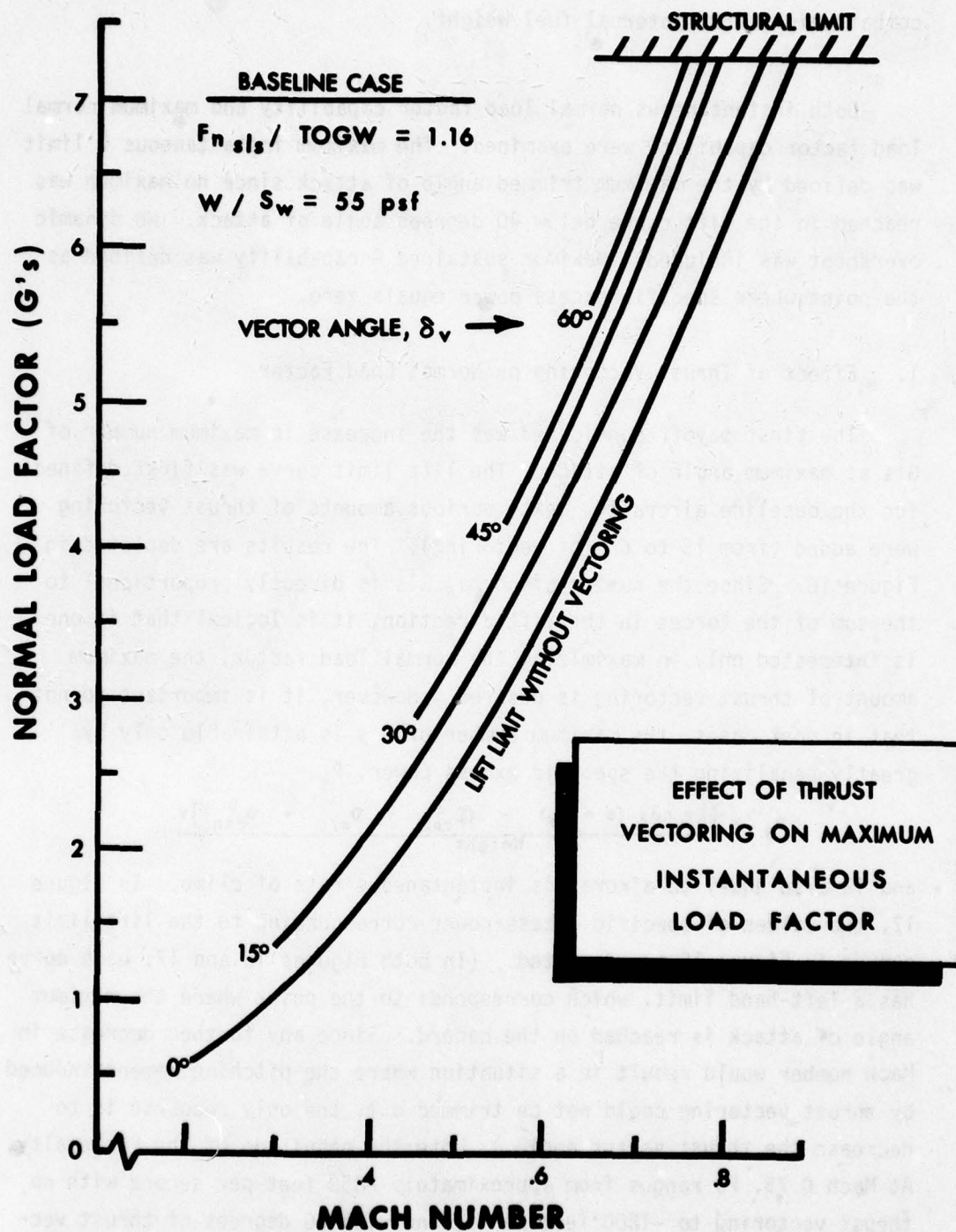


Figure 16. Effect on Instantaneous Normal Load Factor

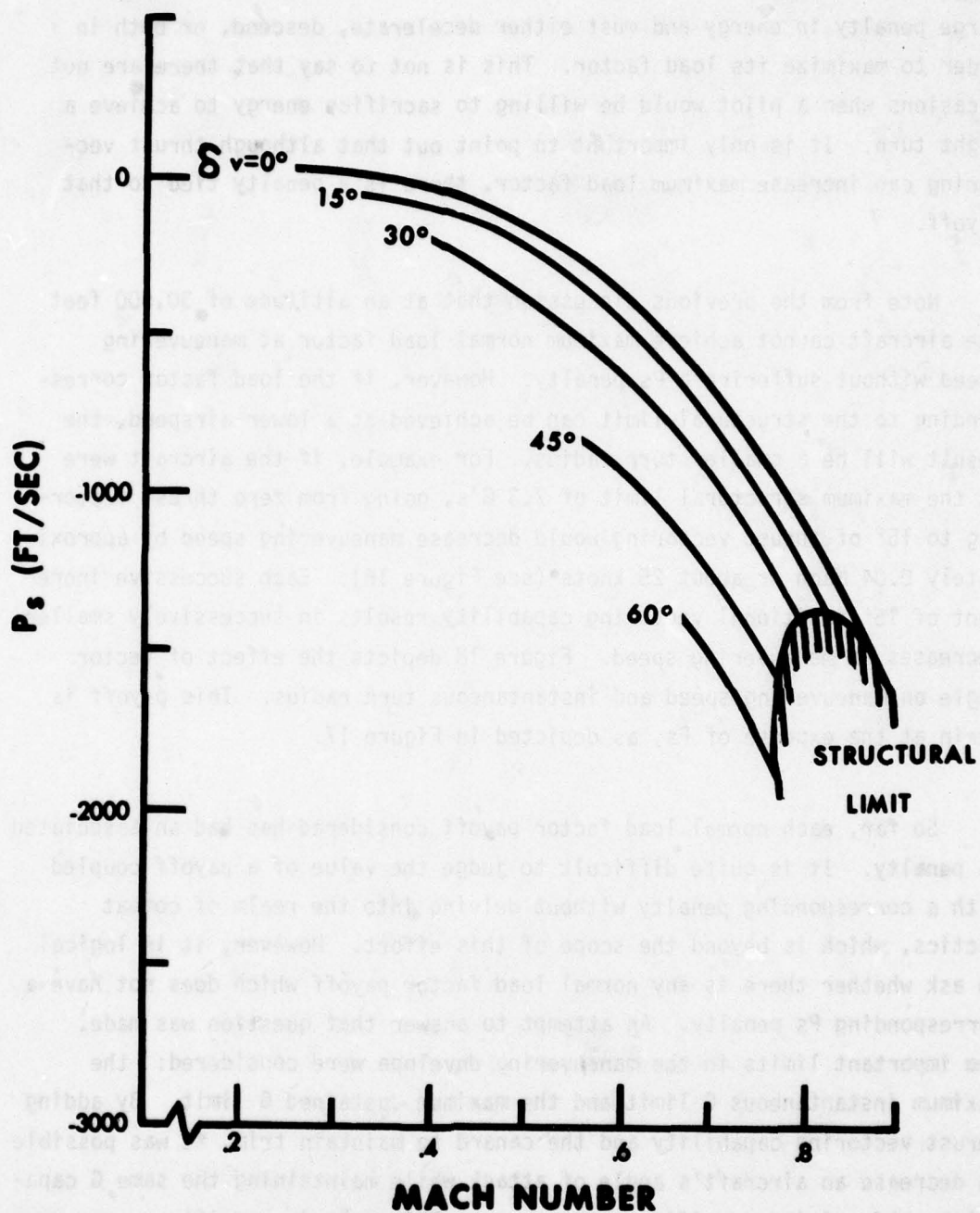


Figure 17. Effect on Specific Excess Power

flight path from 1.1 to 2.4 G's. Therefore, the aircraft must pay a very large penalty in energy and must either decelerate, descend, or both in order to maximize its load factor. This is not to say that there are not occasions when a pilot would be willing to sacrifice energy to achieve a tight turn. It is only important to point out that although thrust vectoring can increase maximum load factor, there is a penalty tied to that payoff.

Note from the previous discussion that at an altitude of 30,000 feet the aircraft cannot achieve maximum normal load factor at maneuvering speed without suffering a P_s penalty. However, if the load factor corresponding to the structural limit can be achieved at a lower airspeed, the result will be a smaller turn radius. For example, if the aircraft were at the maximum structural limit of 7.3 G's, going from zero thrust vectoring to 15° of thrust vectoring would decrease maneuvering speed by approximately 0.04 Mach or about 25 knots (see Figure 16). Each successive increment of 15° additional vectoring capability results in successively smaller decreases in maneuvering speed. Figure 18 depicts the effect of vector angle on maneuvering speed and instantaneous turn radius. This payoff is again at the expense of P_s , as depicted in Figure 17.

So far, each normal load factor payoff considered has had an associated P_s penalty. It is quite difficult to judge the value of a payoff coupled with a corresponding penalty without delving into the realm of combat tactics, which is beyond the scope of this effort. However, it is logical to ask whether there is any normal load factor payoff which does not have a corresponding P_s penalty. An attempt to answer that question was made. Two important limits in the maneuvering envelope were considered: the maximum instantaneous G limit and the maximum sustained G limit. By adding thrust vectoring capability and the canard to maintain trim, it was possible to decrease an aircraft's angle of attack while maintaining the same G capability and gaining specific excess power. This gain in specific excess power could then be traded away for additional normal load factor capability. This was done for various thrust vector angles to determine an optimum thrust vector schedule and the resultant increase in normal load factor capability.

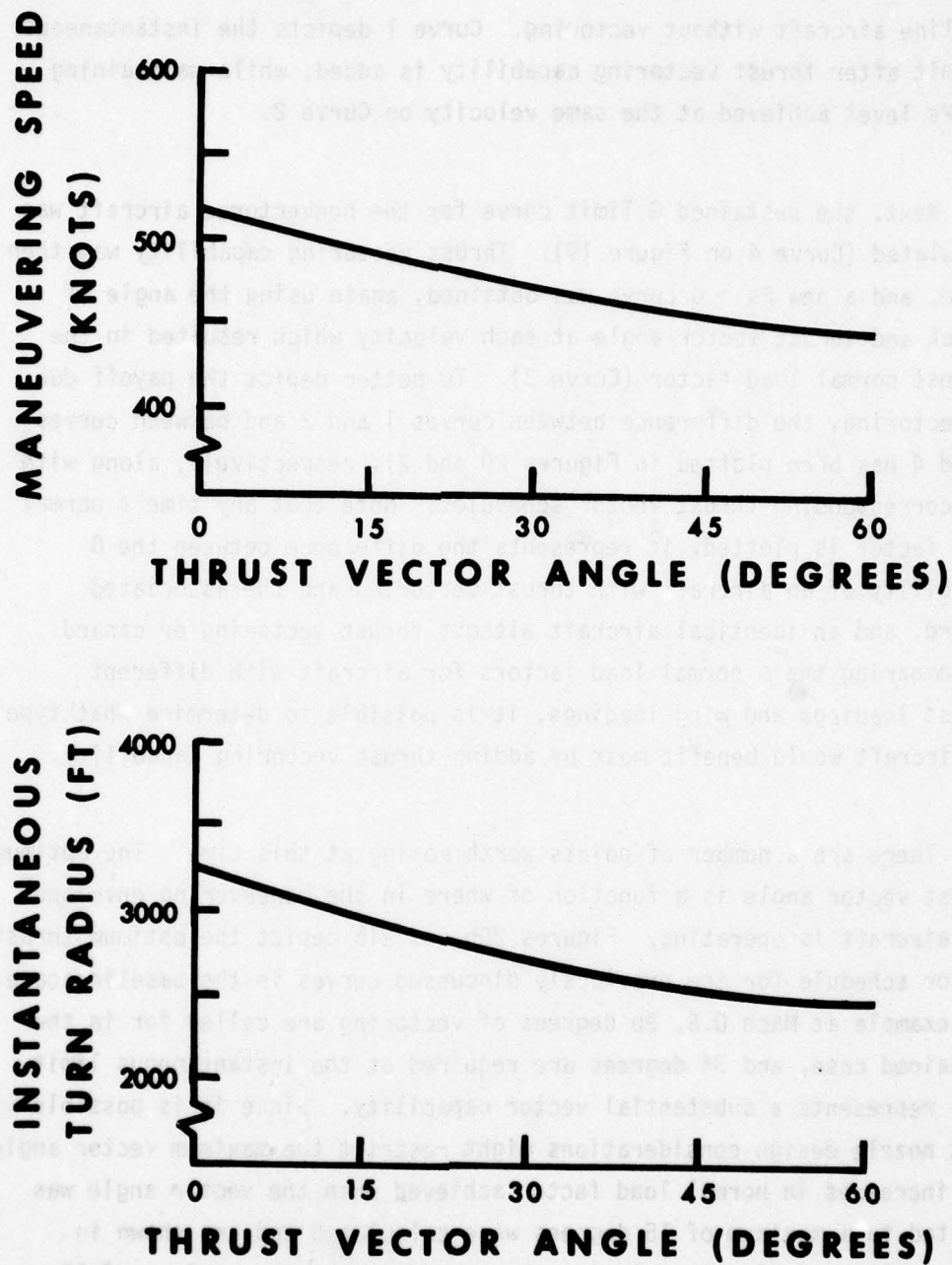


Figure 18. Effect on Maneuver Speed and Turn Radius

Curve 2 in Figure 19 depicts the maximum instantaneous G limit for the baseline aircraft without vectoring. Curve 1 depicts the instantaneous G limit after thrust vectoring capability is added, while maintaining the P_s level achieved at the same velocity on Curve 2.

Next, the sustained G limit curve for the nonvectored aircraft was calculated (Curve 4 on Figure 19). Thrust vectoring capability was then added, and a new $P_s = 0$ curve was obtained, again using the angle of attack and thrust vector angle at each velocity which resulted in the highest normal load factor (Curve 3). To better depict the payoff due to vectoring, the difference between curves 1 and 2 and between curves 3 and 4 has been plotted in Figures 20 and 21, respectively, along with the corresponding thrust vector schedules. Note that any time Δ normal load factor is plotted, it represents the difference between the G capability of an aircraft with thrust vectoring and the associated canard, and an identical aircraft without thrust vectoring or canard. By comparing the Δ normal load factors for aircraft with different thrust loadings and wing loadings, it is possible to determine what type of aircraft would benefit most by adding thrust vectoring capability.

There are a number of points worth noting at this time. The optimum thrust vector angle is a function of where in the maneuvering envelope the aircraft is operating. Figures 20b and 21b depict the optimum thrust vector schedule for the previously discussed curves in the baseline case. For example at Mach 0.8, 20 degrees of vectoring are called for in the sustained case, and 34 degrees are required at the instantaneous limit. This represents a substantial vector capability. Since it is possible that nozzle design considerations might restrict the maximum vector angle, the increases in normal load factor achieved when the vector angle was limited to a maximum of 15 degrees were calculated and are shown in Figures 20a and 21a. Restricting the vector angle to a maximum of 15 degrees decreased the G payoff by about 36% for the instantaneous case and 12% for the sustained case. While considering payoffs due to thrust vectoring that do not result in a P_s penalty, it is worth noting

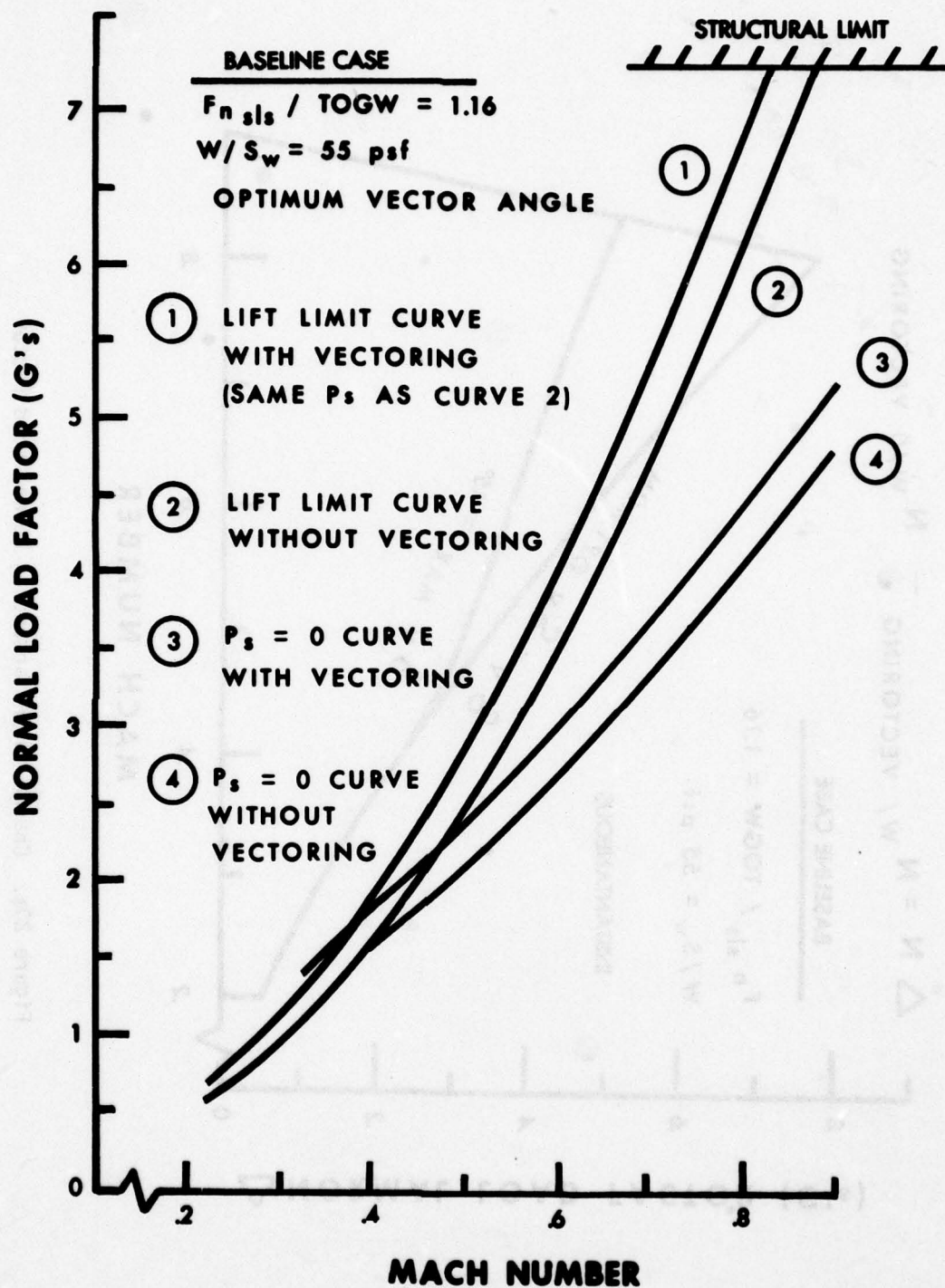
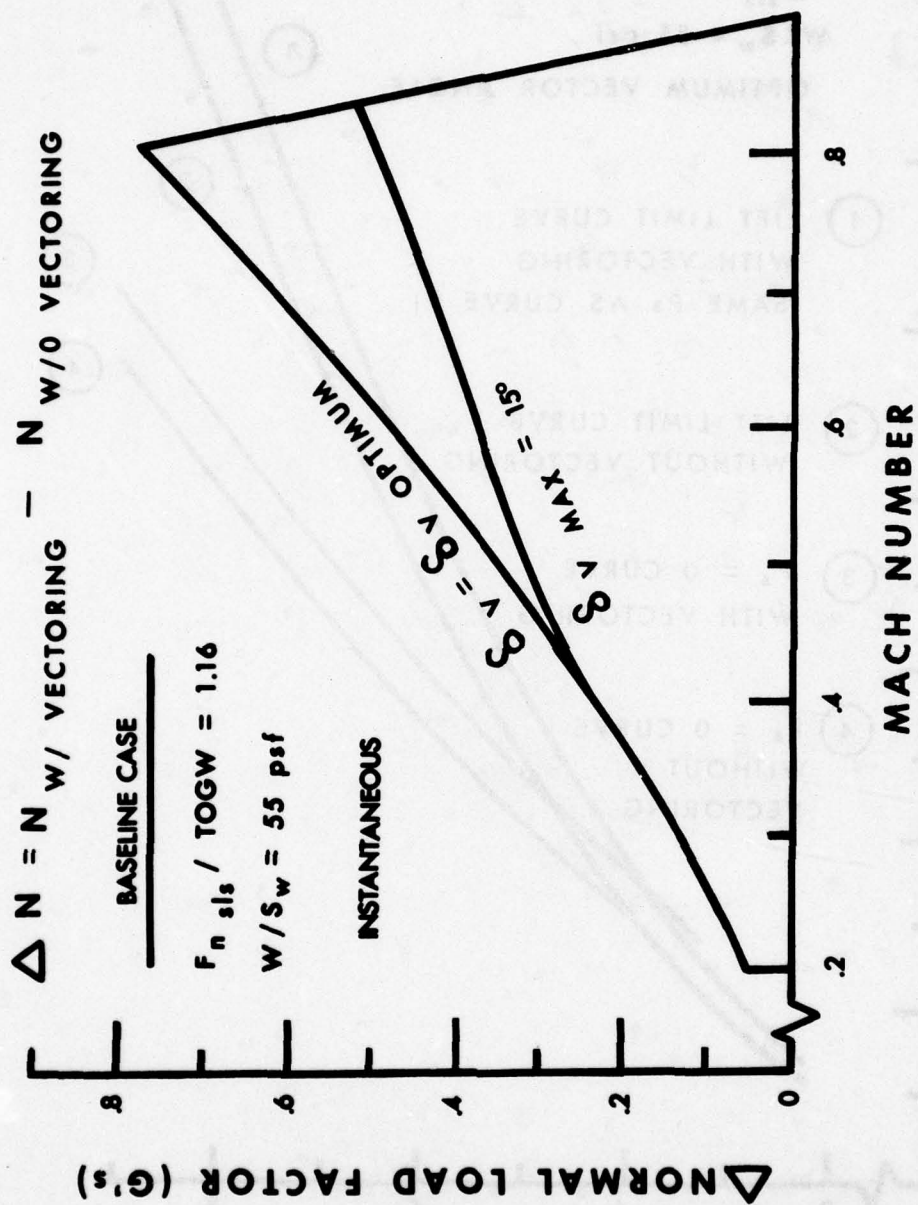


Figure 19. V-N Diagram, Baseline Case



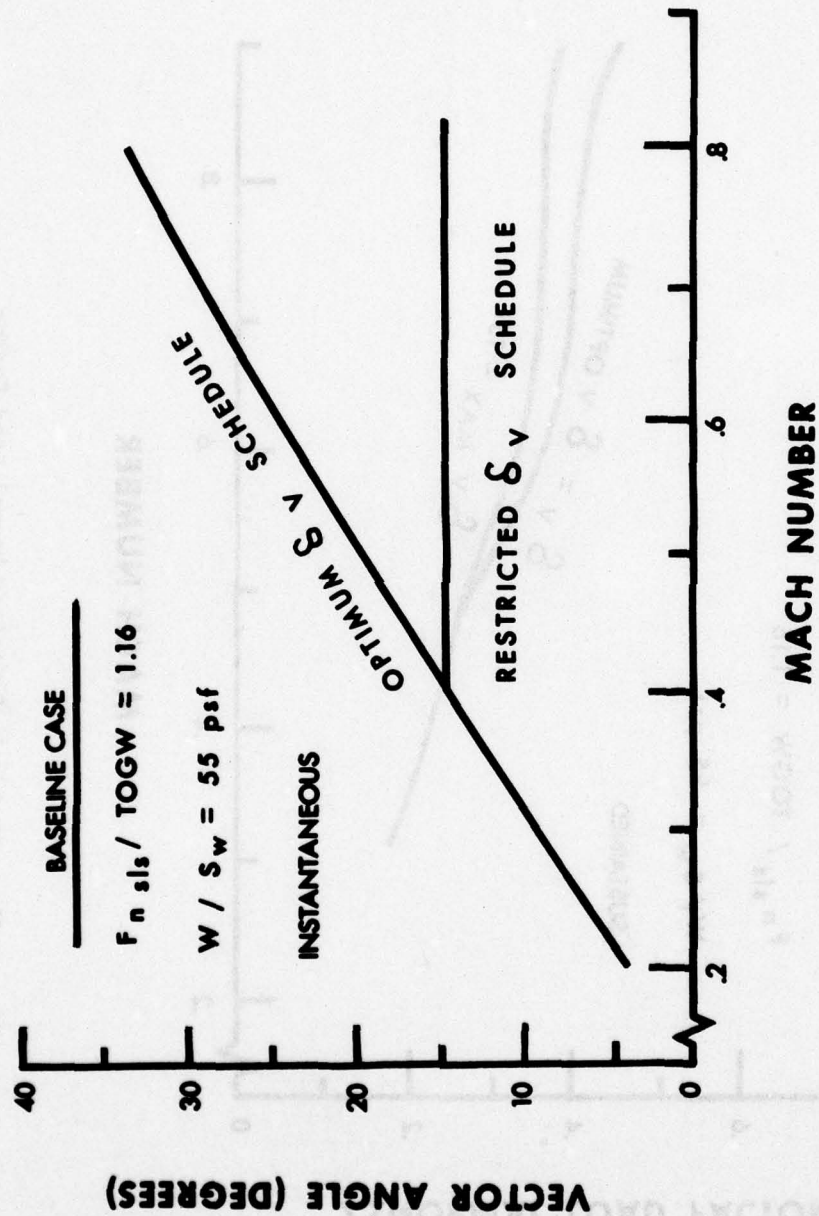


Figure 20b. Thrust Vector Schedule - Instantaneous Turn

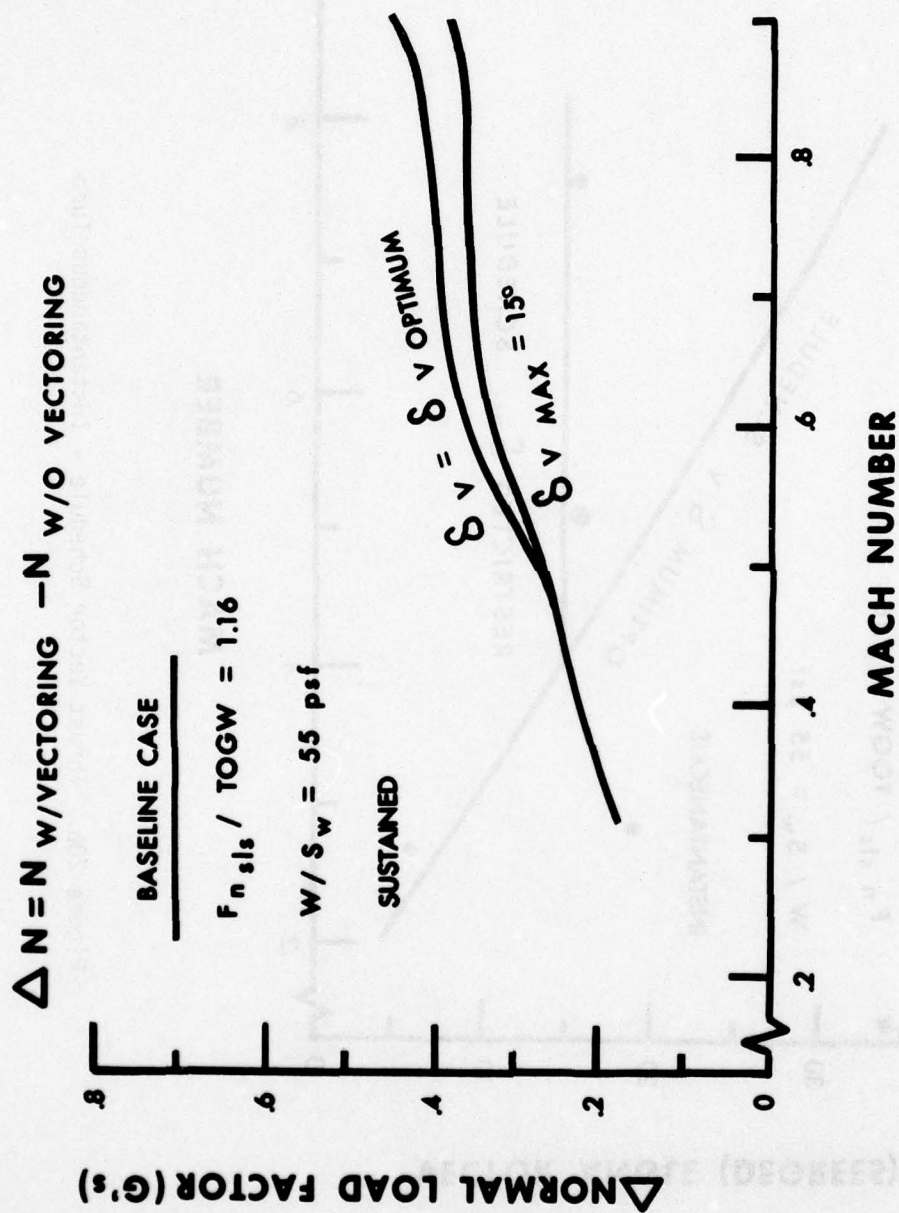


Figure 21a. Change in Sustained Normal Load Factor

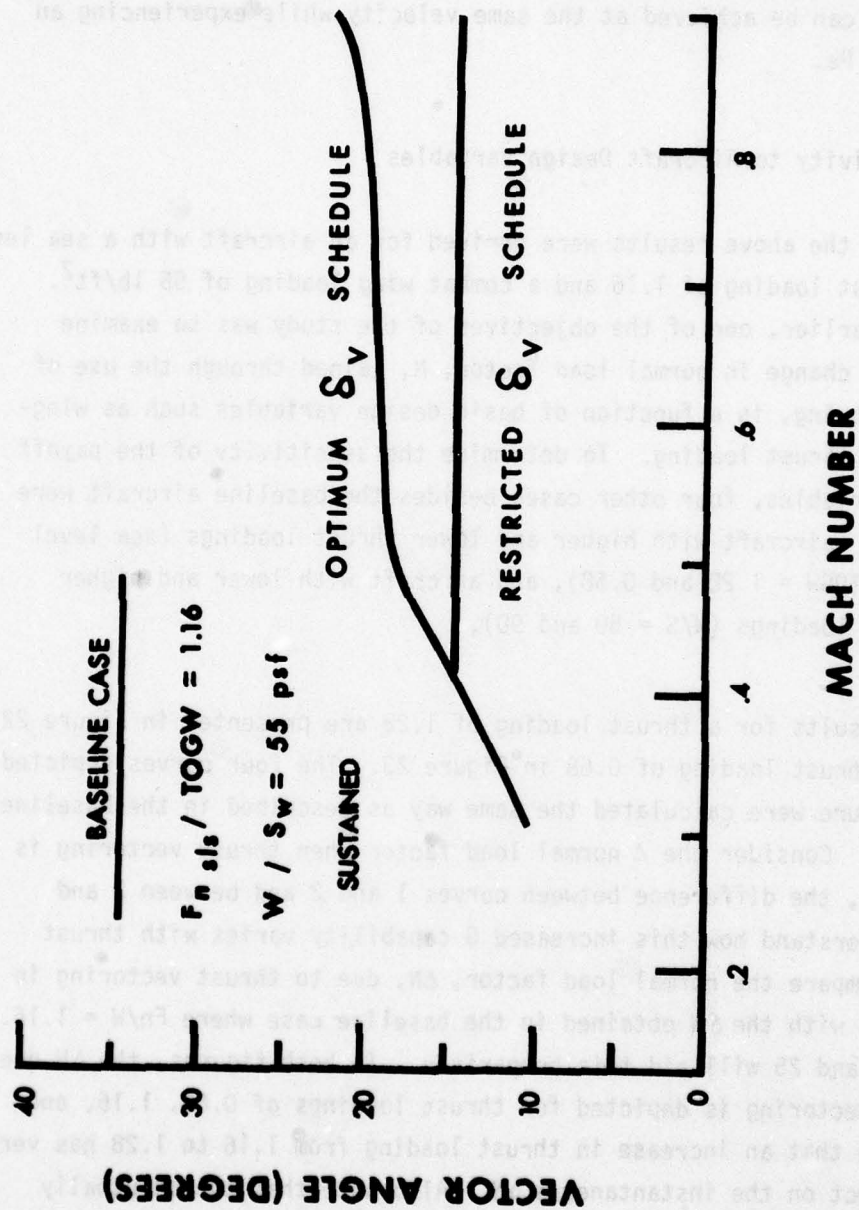


Figure 21b. Thrust Vector Schedules - Sustained Turn

that there are three different ways the results can be viewed: 1) at a given velocity, the addition of thrust vectoring can increase the maximum normal load factor capability at the same P_s ; 2) a given load factor can be achieved at a lower velocity and the same P_s ; 3) the same load factor can be achieved at the same velocity while experiencing an increase in P_s .

2. Sensitivity to Aircraft Design Variables

All of the above results were derived for an aircraft with a sea level static thrust loading of 1.16 and a combat wing loading of 55 lb/ft². As stated earlier, one of the objectives of the study was to examine whether the change in normal load factor, N , gained through the use of thrust vectoring, is a function of basic design variables such as wing-loading and thrust loading. To determine the sensitivity of the payoff to these variables, four other cases besides the baseline aircraft were considered: aircraft with higher and lower thrust loadings (sea level static, $F_n/TOGW = 1.28$ and 0.68), and aircraft with lower and higher combat wing loadings ($W/S = 50$ and 90).

The results for a thrust loading of 1.28 are presented in Figure 22 and for a thrust loading of 0.68 in Figure 23. The four curves depicted in each figure were calculated the same way as described in the baseline case above. Consider the Δ normal load factor when thrust vectoring is added (i.e., the difference between curves 1 and 2 and between 3 and 4). To understand how this increased G capability varies with thrust loading, compare the normal load factor, ΔN , due to thrust vectoring in these cases with the ΔN obtained in the baseline case where $F_n/W = 1.16$. Figures 24 and 25 will aid this comparison. In both figures, the ΔN due to thrust vectoring is depicted for thrust loadings of 0.68, 1.16, and 1.28. Note that an increase in thrust loading from 1.16 to 1.28 has very little effect on the instantaneous ΔN . Also note that the ΔN usually decreases to zero somewhere above Mach 0.8. This is due to the fact that the structural limit has been reached for the nonvectored case,

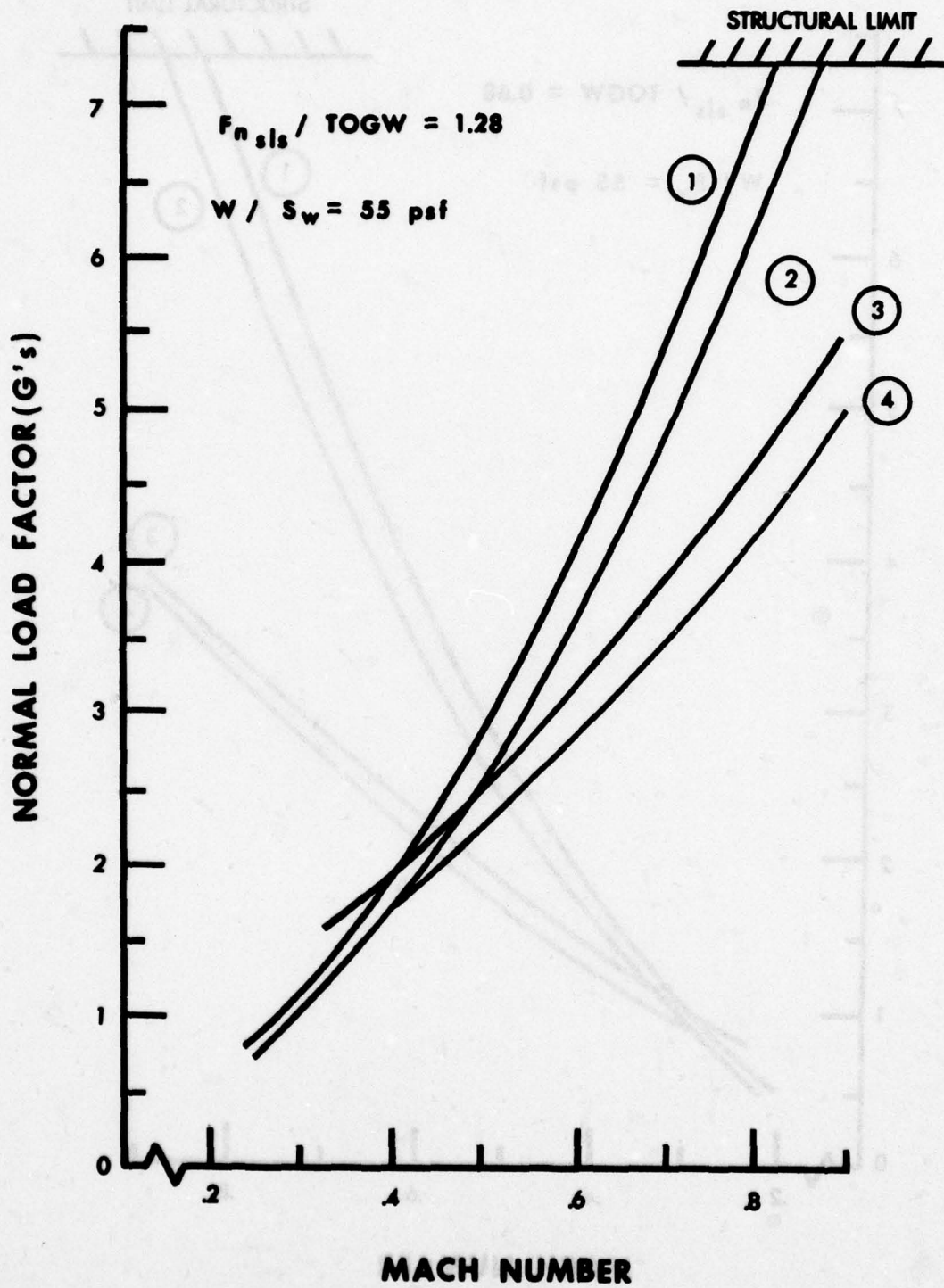


Figure 22. V-N Diagram - Increased Thrust Loading

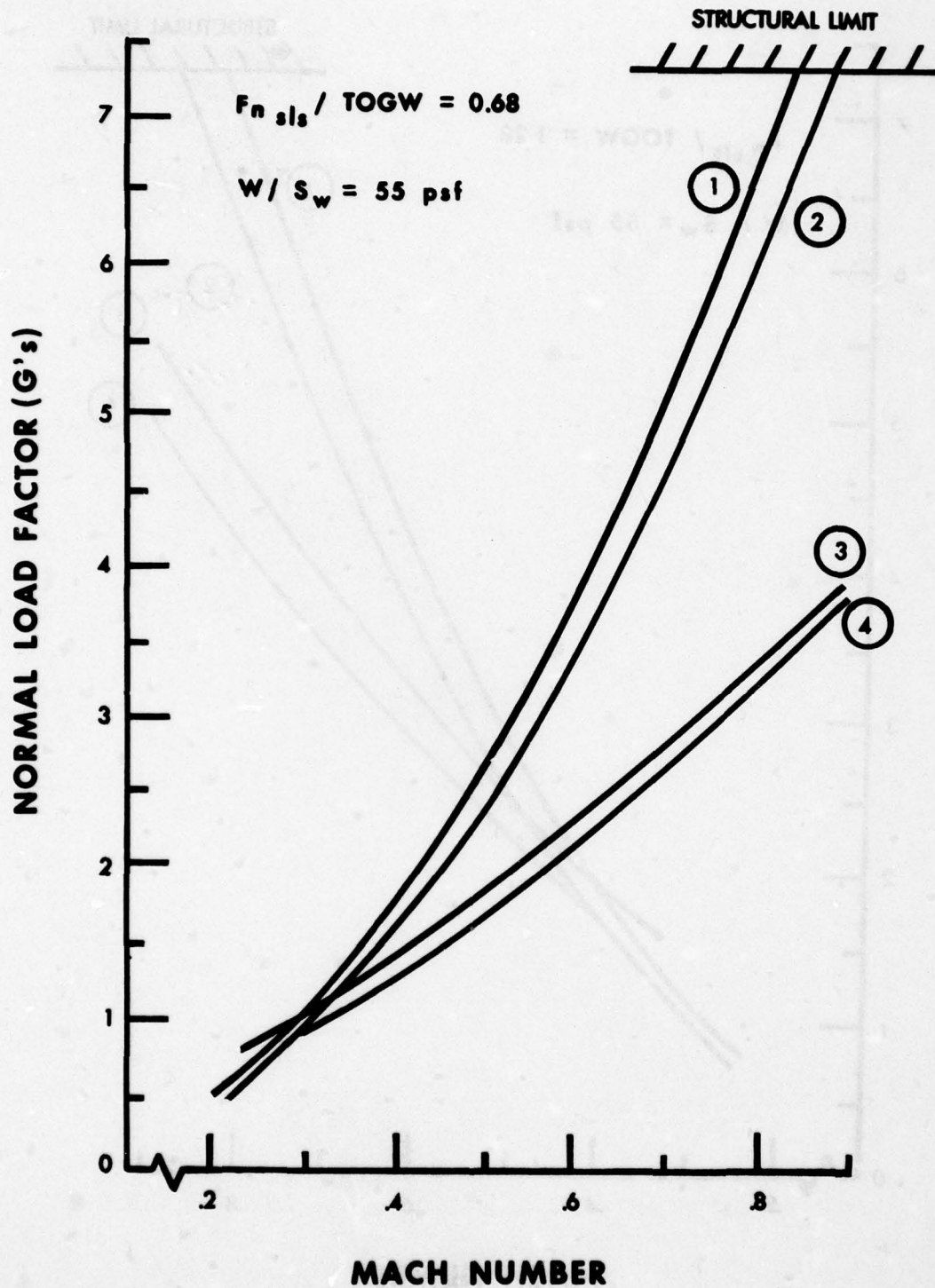


Figure 23. V-N Diagram - Decreased Thrust Loading

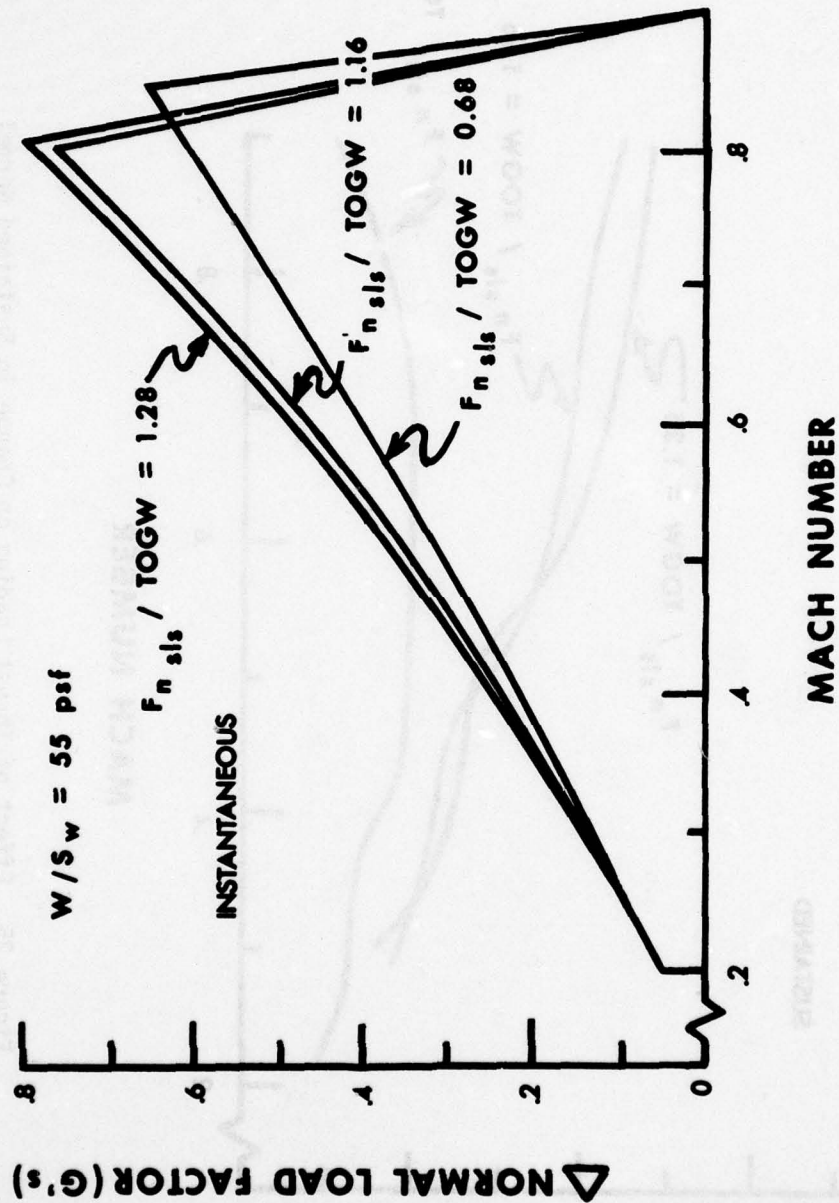


Figure 24. Effect of Thrust Loading on Change in Instantaneous Normal Load Factor

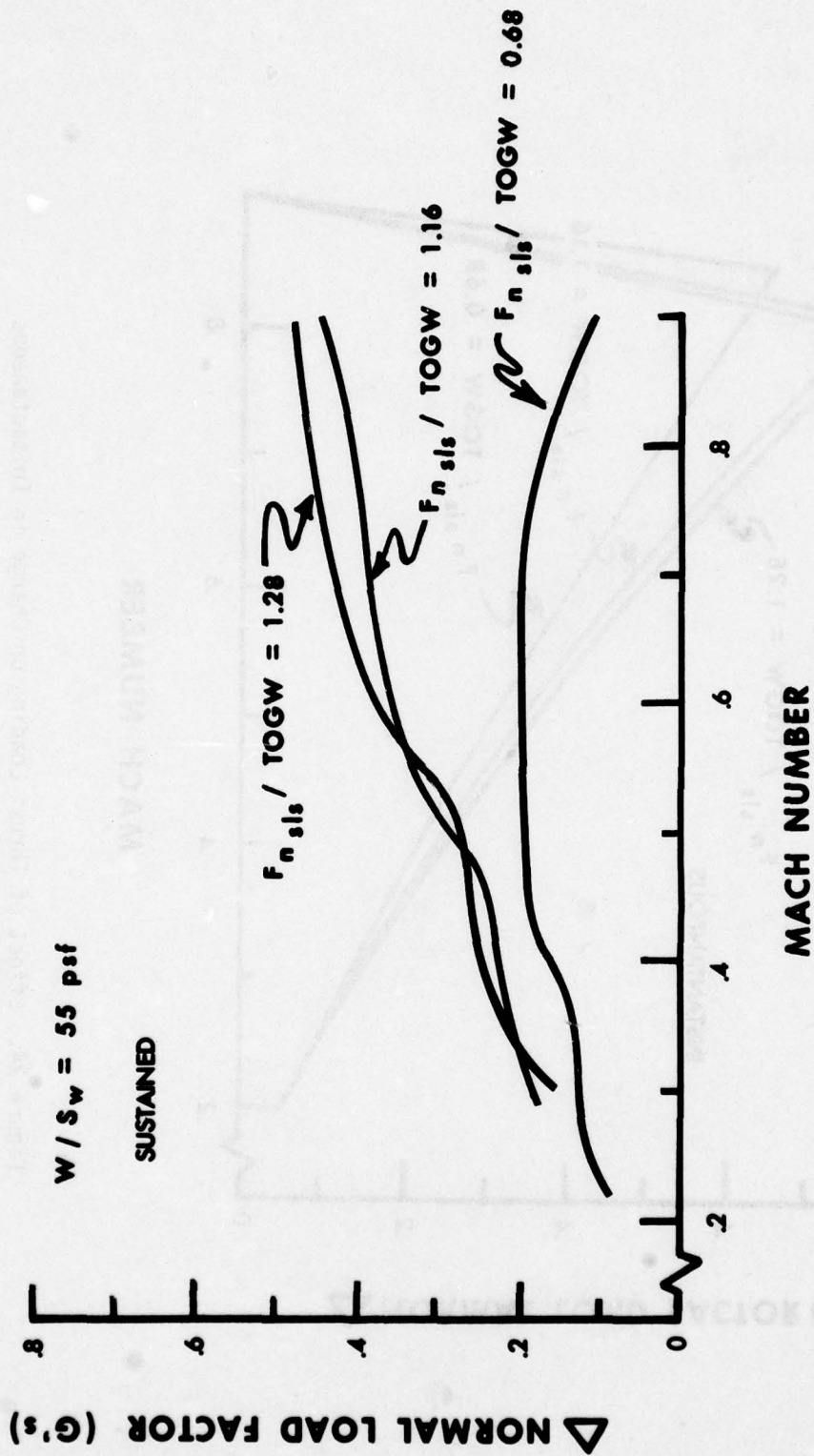


Figure 25. Effect of Thrust Loading on Change in Sustained Normal Load Factor

and any additional increase in load factor is prohibited. If it were not for the structural limit, the ΔN due to vectoring would continue to increase. Since the structural limit has been reached, and additional lift is available due to vectoring, the aircraft angle of attack could be reduced, thus reducing induced drag and thereby increasing P_s . It is also evident from Figures 24 and 25 that the maximum sustained G capability is more sensitive to thrust loading than is instantaneous G capability. The sensitivity of ΔN payoff to thrust loading is more easily seen in the case of the more significant change in thrust loading achieved by reducing it to a value of 0.68. Note the magnitude of the sustained ΔN . At its maximum, the payoff is still less than 0.2G, and this small payoff is further reduced as the Mach number increases. The trend of decreased ΔN with reduced thrust loading makes sense. Since thrust is being vectored to produce a force in the lift direction, it is logical that less thrust available for vectoring would result in a smaller payoff.

The baseline aircraft in this study had a combat wing loading of 55. To determine the sensitivity of thrust vectoring benefits to wing loading, cases were examined with wing loadings of 50 and 90, the results of which are presented in Figures 26 and 27, respectively; the resulting ΔN can be more closely examined in Figures 28 and 29. It is interesting to note that reducing wing loading from 55 to 50 results in almost the same instantaneous G capability without vectoring as the baseline case with vectoring (compare Curve 1 on Figure 19 with Curve 2 on Figure 26). Comparing Curve 3 on Figure 19 with Curve 4 on Figure 26 shows that lowering wing loading to 50 without adding thrust vectoring capability achieves about half the normal load factor increase achieved by adding vectoring capability to the baseline aircraft. Figures 28 and 29 show that the ΔN to be gained is not significantly changed when reducing wing loading from 55 to 50. Note that this reduction in wing loading results in a very slight increase in instantaneous ΔN , but generally a slight decrease in sustained ΔN .

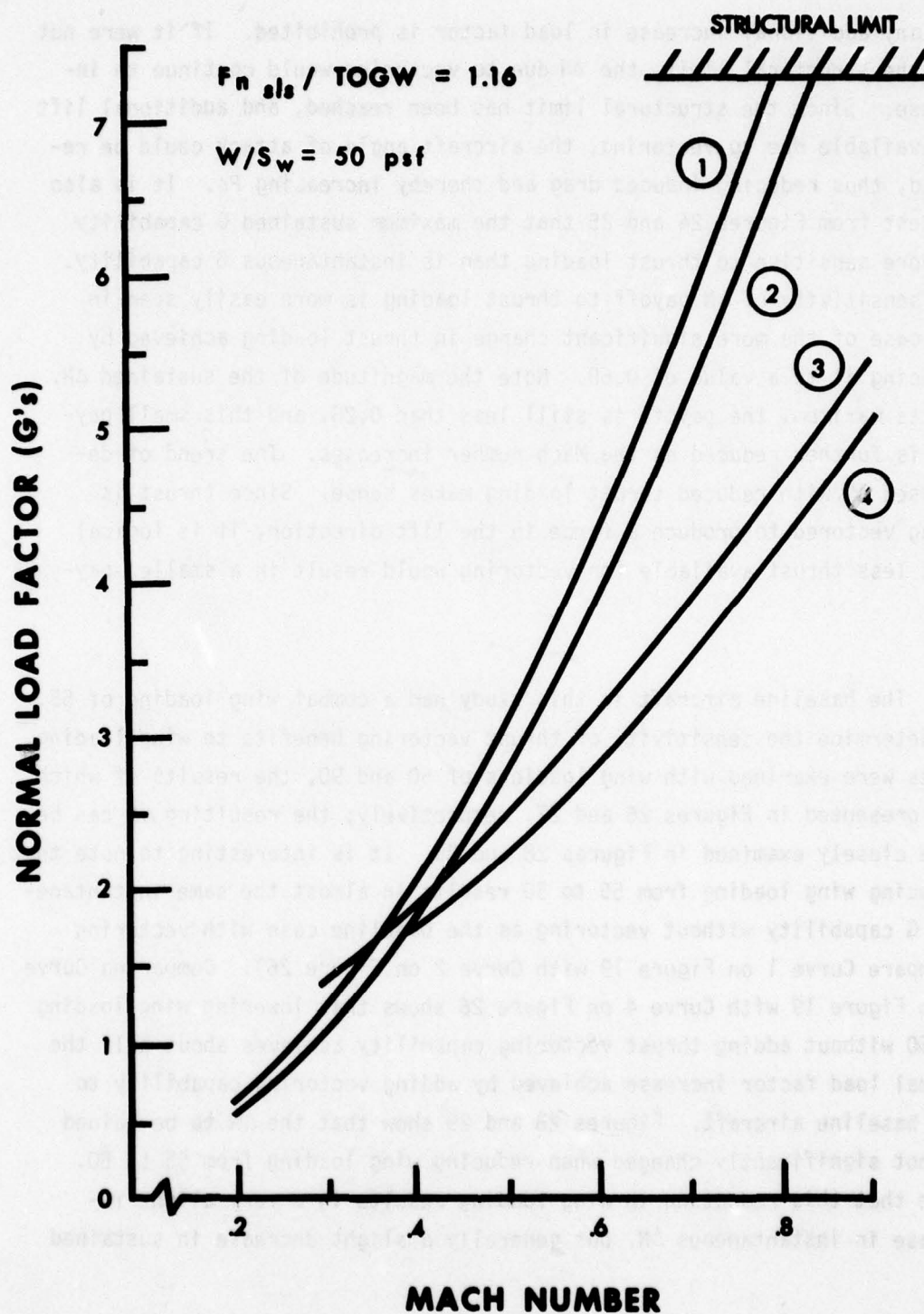


Figure 26. V-N Diagram - Decreased Wing Loading

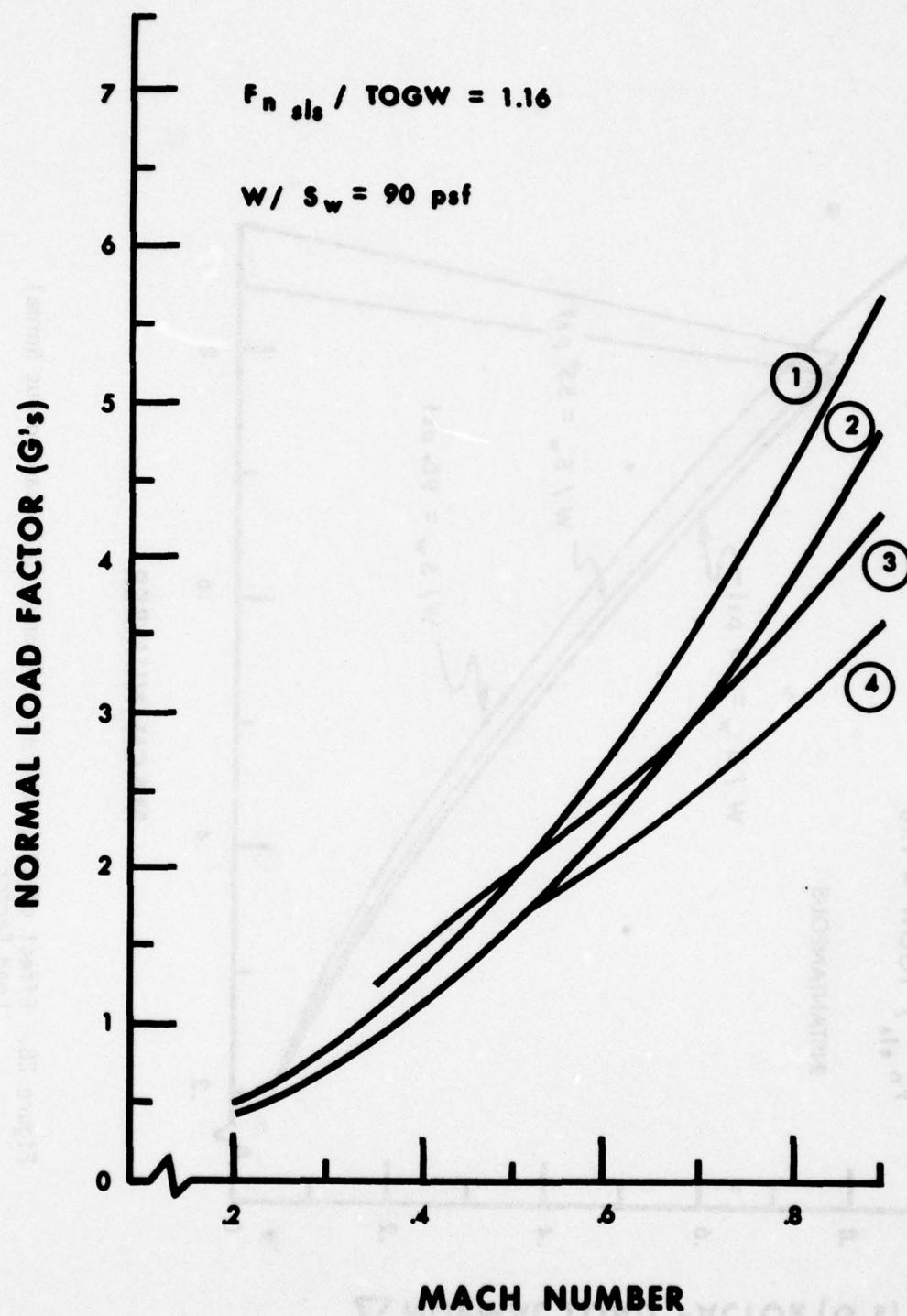


Figure 27. V-N Diagram - Increased Wing Loading

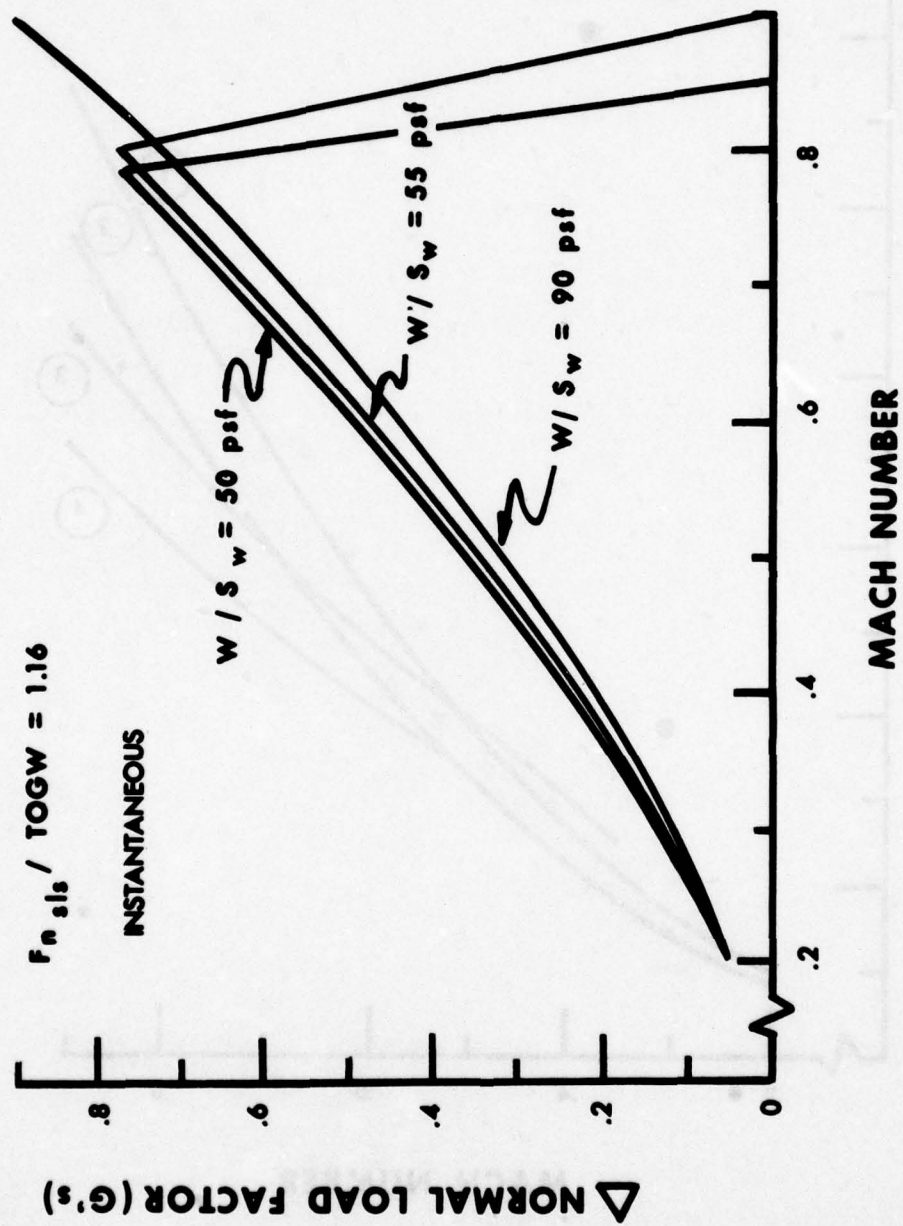


Figure 28. Effect of Wing Loading on Change in Instantaneous Normal Load Factor

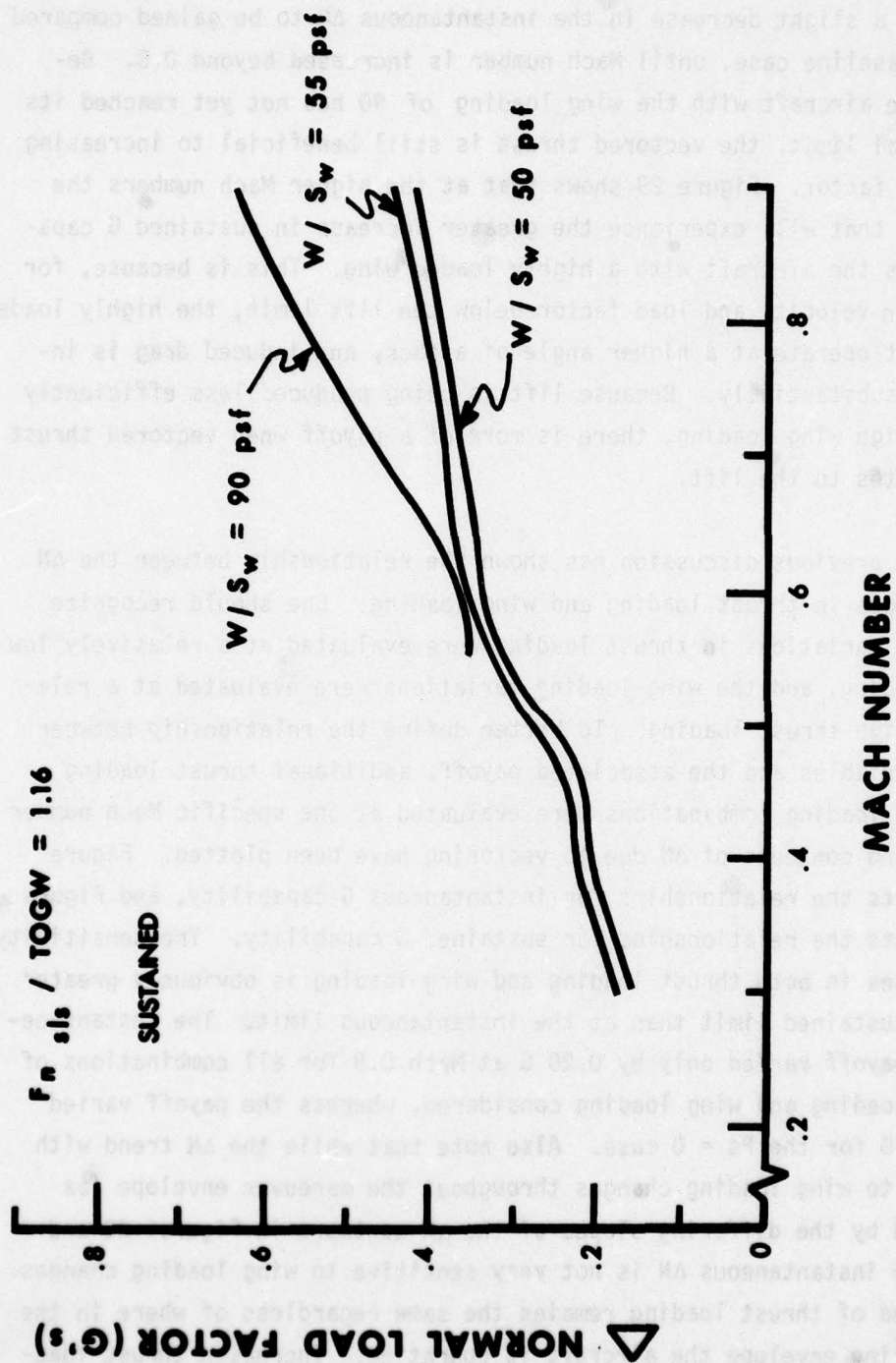


Figure 29. Effect of Wing Loading on Change in Sustained Normal Load Factor

Figure 27 depicts the V-N diagram for a wing loading of 90. Figure 28 shows a slight decrease in the instantaneous ΔN to be gained compared to the baseline case, until Mach number is increased beyond 0.8. Because the aircraft with the wing loading of 90 has not yet reached its structural limit, the vectored thrust is still beneficial to increasing the load factor. Figure 29 shows that at the higher Mach numbers the aircraft that will experience the greater increase in sustained G capability is the aircraft with a highly loaded wing. This is because, for any given velocity and load factor below the lift limit, the highly loaded wing must operate at a higher angle of attack, and induced drag is increased substantially. Because lift is being produced less efficiently with a high wing loading, there is more of a payoff when vectored thrust contributes to the lift.

The previous discussion has shown the relationship between the ΔN and changes in thrust loading and wing loading. One should recognize that the variations in thrust loading were evaluated at a relatively low wing loading, and the wing loading variations were evaluated at a relatively high thrust loading. To better define the relationship between these variables and the associated payoff, additional thrust loading and wing loading combinations were evaluated at one specific Mach number (0.8), and contours of ΔN due to vectoring have been plotted. Figure 30 depicts the relationships for instantaneous G capability, and Figure 31 depicts the relationships for sustained G capability. The sensitivity to changes in both thrust loading and wing loading is obviously greater at the sustained limit than at the instantaneous limit. The instantaneous ΔN payoff varied only by 0.20 G at Mach 0.8 for all combinations of thrust loading and wing loading considered, whereas the payoff varied by 0.47 G for the $P_s = 0$ case. Also note that while the ΔN trend with respect to wing loading changes throughout the maneuver envelope (as depicted by the differing slopes of the ΔN contours in Figures 30 and 31), the instantaneous ΔN is not very sensitive to wing loading changes. The trend of thrust loading remains the same regardless of where in the maneuvering envelope the aircraft is operating. Increased thrust loading always results in increased Δ normal load factor payoff.

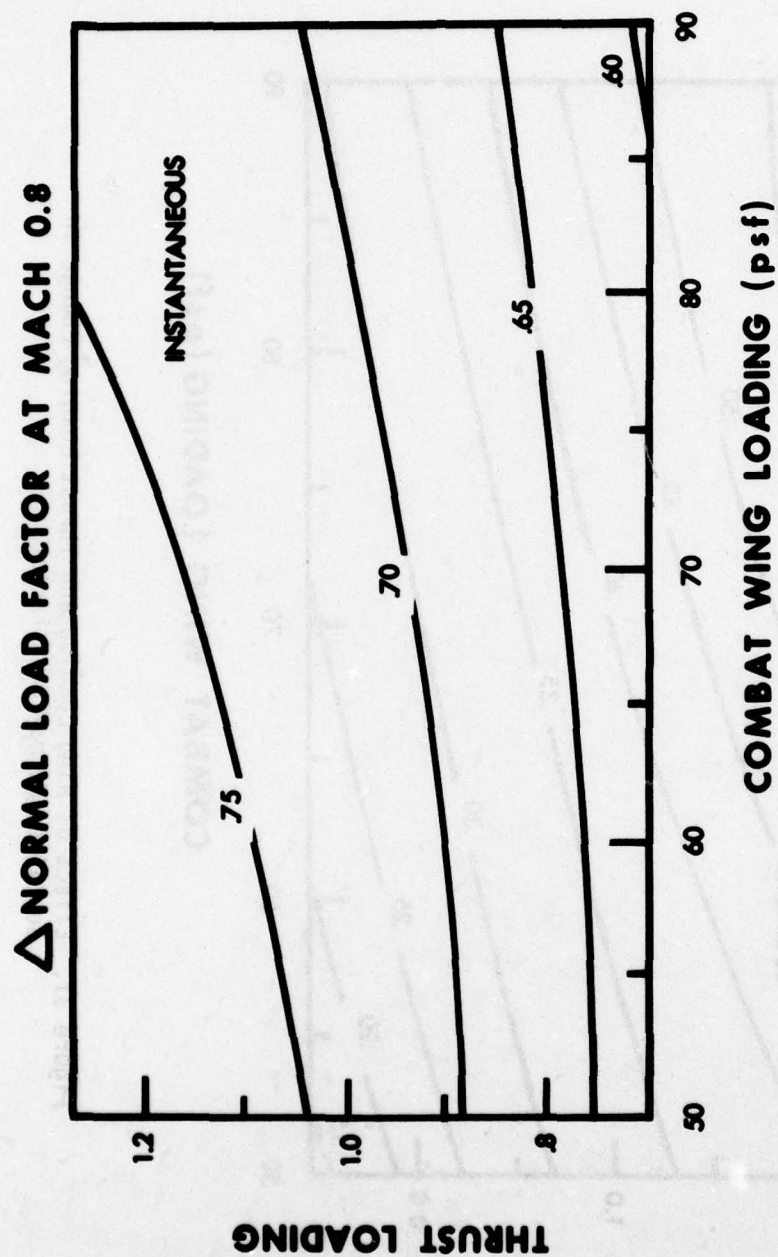


Figure 30. Effect of Wing Loading and Thrust Loading Change in Instantaneous Normal Load Factor

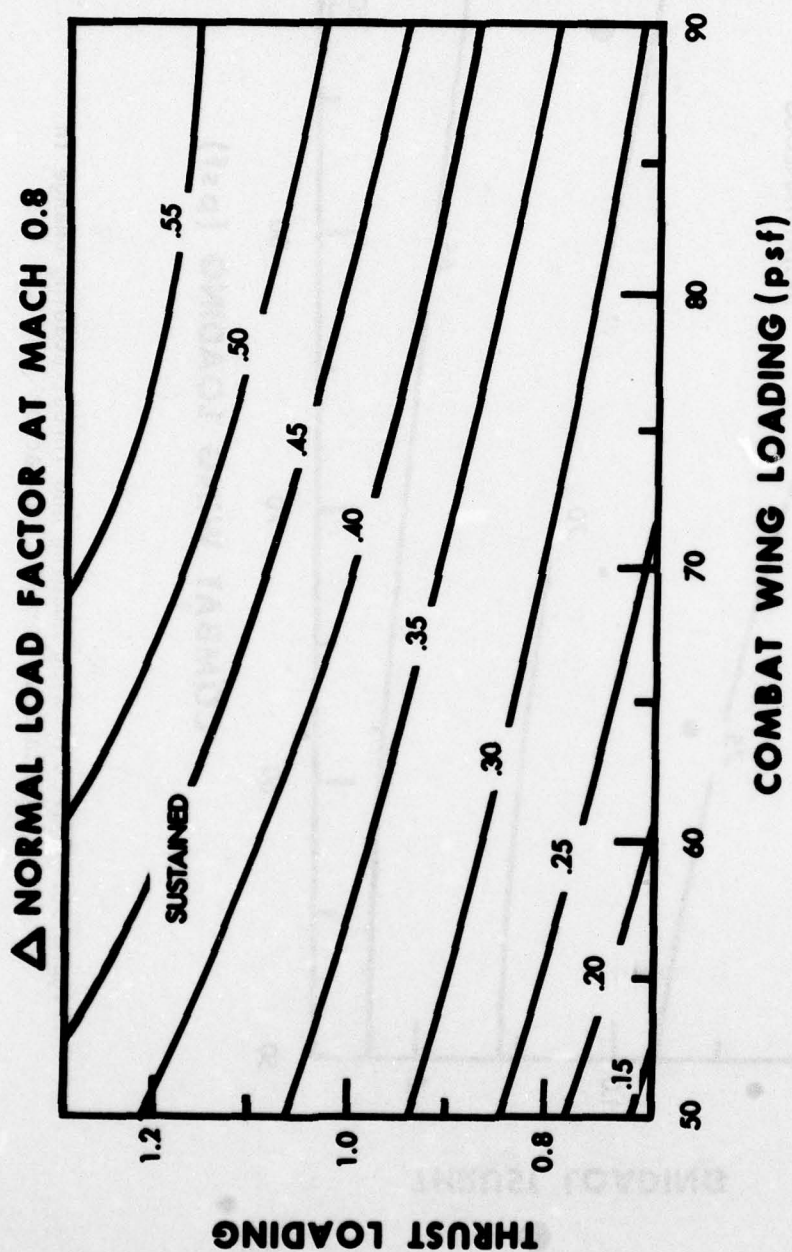


Figure 31. Effect of Wing Loading and Thrust Loading Change in Sustained Normal Load Factor

Figures 32 and 33 depict the optimum thrust vector angles corresponding to the ΔN payoffs at Mach 0.8 depicted in Figures 30 and 31, respectively. Note that for maximum instantaneous G capability, very large vector angles are required (up to 50 degrees). To determine how dependent this payoff is on achieving these large vector angles, the ΔN payoff for 15 degrees of vectoring was examined. Limiting vector angle to 15 degrees would reduce the ΔN payoffs in Figure 20a by a maximum of 0.33 G's and a minimum of 0.21 G's. This would represent a relatively significant decrease in payoff. Figures 33 and 21b show that smaller vector angles are required at the maximum sustained limit (optimum deflection angle ranged from 15 to 28 degrees). Since the optimum deflection angle is smaller for the maximum sustained case, restricting the deflection to 15 degrees had a reduced effect. The ΔN payoffs depicted in Figure 21a would be decreased by a maximum of 0.13 G's and a minimum of 0 G's.

Before drawing any conclusions on the relative value of thrust vectoring, other alternatives should be examined. In this study, the lift from the canard was responsible for about 2/3 of the increase in G capability. This fraction would naturally change with changes in canard design and location. But practical considerations place restrictions on canard design and placement, and it is easy to conclude that the canard lift is likely to be at least of the same magnitude as the force resulting from thrust vectoring. For this reason, it would be wise to explore the option of simply adding a canard without any thrust vectoring capability. The canard could be used to trim the wing pitching moment and thus reduce the downward force produced by the horizontal stabilizer. With a canard and horizontal stabilizer both operating at the proper positive angle of attack, the aircraft could be trimmed and at the same time experience a normal load factor payoff resulting from the lift produced by the canard and horizontal stabilizer. The net result would be to effectively decrease the wing loading of the aircraft (by supplementing lift with canard and horizontal stabilizer lift). This suggests another alternative which should be considered: decreasing wing loading by increasing the size of the wing. Obviously the selection of the

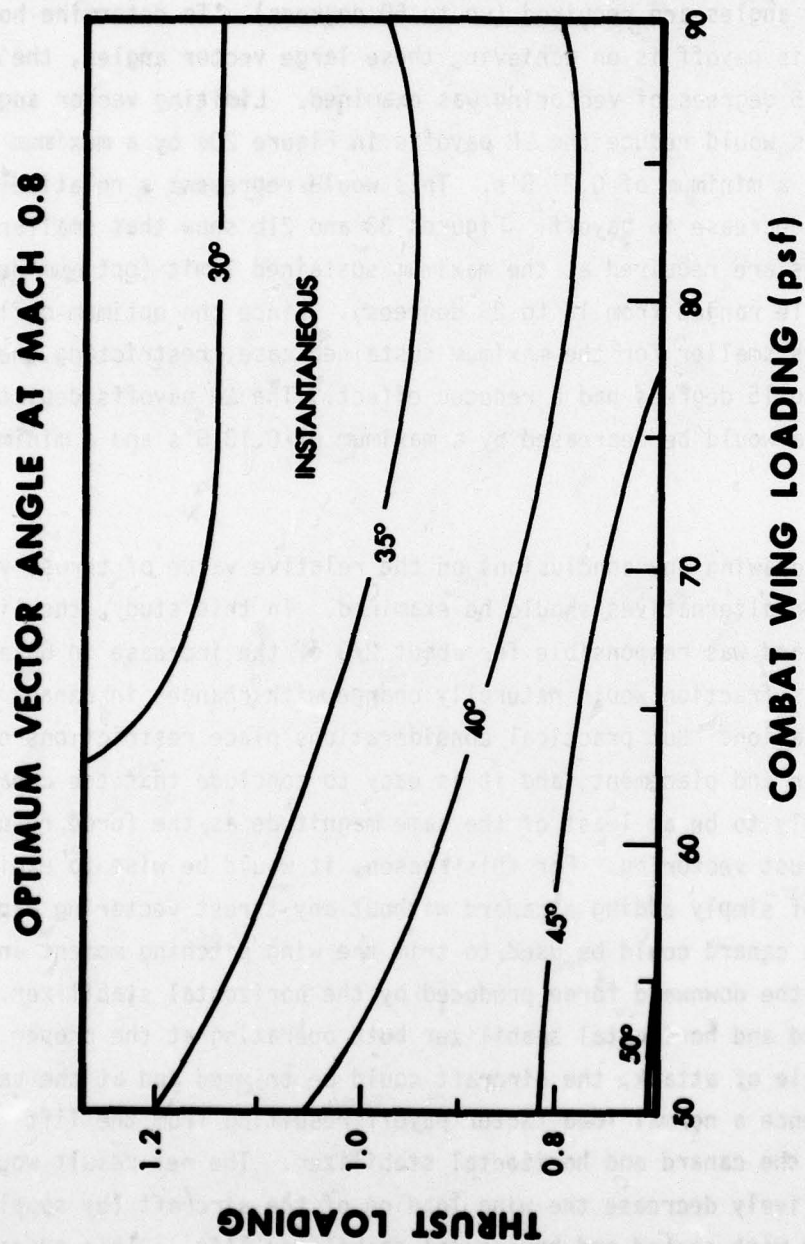


Figure 32. Effect of Wing Loading and Thrust Loading on Vector Angle in Instantaneous Turn

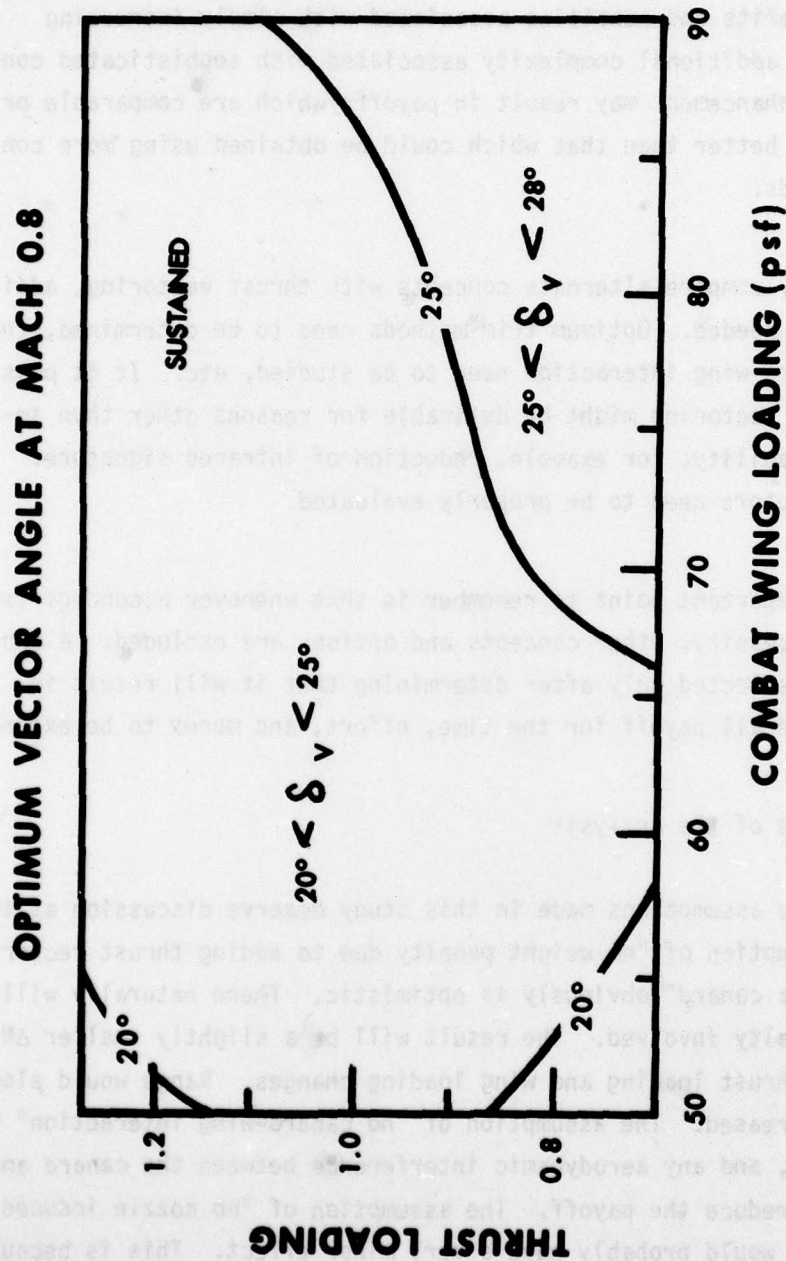


Figure 33. Effect of Wing Loading and Thrust Loading on Vector Angle in Sustained Turn

desired wing loading is affected by many factors in addition to desired turning performance. But it is important to weigh any benefits and penalties associated with concepts which effectively reduce wing loading against the benefits and penalties associated with simply increasing wing size. The additional complexity associated with sophisticated concepts of lift enhancement may result in payoffs which are comparable or only marginally better than that which could be obtained using more conventional methods.

To properly compare alternate concepts with thrust vectoring, additional study is needed. Optimum trim methods need to be determined, the effects of canard-wing interaction need to be studied, etc. It is possible that thrust vectoring might be desirable for reasons other than improved maneuverability; for example, reduction of infrared signature. All of these factors need to be properly evaluated.

The most important point to remember is that whenever a concept is selected, by necessity, other concepts and options are excluded. A concept should be selected only after determining that it will result in the greatest overall payoff for the time, effort, and money to be expended.

3. Limitations of the Analysis

Some of the assumptions made in this study deserve discussion at this time. The assumption of "no weight penalty due to adding thrust vectoring capability and a canard" obviously is optimistic. There naturally will be a weight penalty involved. The result will be a slightly smaller ΔN payoff due to thrust loading and wing loading changes. Range would also be slightly decreased. The assumption of "no canard-wing interaction" is also optimistic, and any aerodynamic interference between the canard and the wing would reduce the payoff. The assumption of "no nozzle induced drag reduction" would probably have a very minor effect. This is because any resulting drag reduction would most likely represent a small fraction of the total drag at the high angles of attack encountered in the study.

The effect of assuming "no nozzle induced lift enhancement" is unknown. One of the few pessimistic assumptions was that of trim technique. It was assumed that the wing induced pitching moment would be trimmed with the horizontal tail and that the pitching moment induced by thrust vectoring would be trimmed with the canard. It is recognized that this is not the optimum way to trim the aircraft. It would probably be advantageous to use either the canard or vectoring capability to trim the wing, thereby decreasing or eliminating the downward force required by the horizontal stabilizer. Exploring alternate trim techniques was beyond the scope of this study, however. There are many other aspects of the problem that have not been considered, such as possible control system problems and stability or controllability problems at low Mach numbers. Another limitation of the study is that only one altitude was considered. It is possible that the higher thrust available at lower altitudes may increase the payoff due to thrust vectoring. However, it should be remembered that the nonvectored aircraft's performance would also be improved at lower altitudes, and the relative advantage that thrust vectoring may offer could be reduced. Higher altitudes result in degraded turning performance, which may make some form of lift enhancement look attractive, but higher altitudes also result in decreased thrust available to vector.

The scope of the study was also limited by the fact that only one maneuver was studied a maximum power level turn. Although many of the trends noted would hold true for other maneuvers, it is possible that other maneuvers could show either increased or decreased payoff due to thrust vectoring. No consideration was given to the concept of in-flight thrust reversal, which could result in a payoff by allowing the pilot to make rapid airspeed changes and providing him with the means to force an overshoot in combat.

4. Conclusions Regarding Thrust Vectoring

This study was admittedly a simplified one but should be sufficient to define the first-order effects. The following conclusions are general trends noted from the study. Deviations from these trends may occur at very low Mach numbers.

1. Thrust vectoring enhances maximum instantaneous G capability more than maximum sustained G capability. However, the substantially greater benefit at the lift limit is highly dependent on the ability to achieve large vector angles.
2. Sustained G capability is more sensitive than instantaneous G capability to changes in either thrust loading or wing loading.
3. ΔN generally increases with Mach number until the structural limit is reached. At this point, there is no longer any payoff from a ΔN standpoint. However, there is a small P_s payoff.
4. As thrust loading is decreased, the thrust vector angle must be increased to maximize instantaneous G capability.
5. Instantaneous ΔN payoff due to vectoring is relatively insensitive to wing loading changes.
6. Maximum sustained ΔN payoff due to vectoring is slightly higher for aircraft with higher wing loadings.
7. ΔN payoff always increases with increased thrust loading.
8. The optimum vector angle required for maximum instantaneous G capability is much higher than that for sustained G capability.
9. A substantial portion of the increase in G capability (both instantaneous and sustained) results from the canard alone.

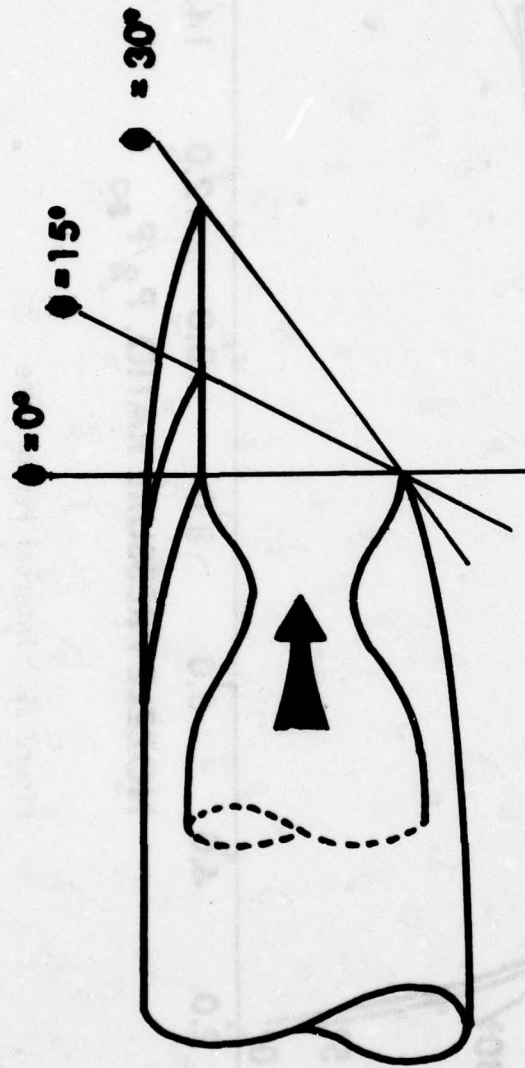
How much ΔN payoff is necessary to warrant serious consideration of a concept is subject to debate. This study indicated that at 30,000 feet the highest increase in instantaneous G capability due to vectoring without incurring an additional P_s penalty was around 0.8 G's and the highest increase in sustained G capability was around 0.55 G's. Depending on thrust loading and wing loading, this payoff was often considerably less. One should remember that the magnitude of this payoff is dependent on both the assumptions previously made and on the ability to achieve large vector angles. The payoff achieved in actual practice could quite possibly be smaller.

SECTION VI

FORCE ACCOUNTING PROCEDURES

Traditionally, it has been possible to treat gross thrust as a vector whose orientation was aligned with the axis of the nozzle and remained so aligned during variations in nozzle pressure ratio. For some non-axisymmetric nozzle types and vectoring schemes, such a treatment of gross thrust is not valid. As an example, consider a family of single ramp expansion nozzles formed by extending an axisymmetric or two-dimensional configuration as depicted in Figure 34. While the momentum terms of all of those nozzles are aligned with the nozzle axis, the direction of the pressure area term varies with the orientation of the exit plane, and therefore the magnitude and direction of the gross thrust vector varies with the nozzle pressure ratio. It is only because the vector representing the pressure area term and the vector representing the momentum term have traditionally been collinear that in the past it has been possible to reduce the vector expression for gross thrust to a single vector invariant in direction. Figure 35 and 36 depict how gross thrust varies in magnitude and direction as a function of nozzle pressure ratio, respectively, with changes in exit plane orientation. These calculations were based on the ideal case of constant internal area ratio, no internal losses, and an internal contour which results in horizontal flow at the exit. Note that the force applied in the axial or horizontal direction is independent of exit area orientation, and at the design pressure ratio the total force applied is independent of exit area orientation. However, at all other pressure ratios, the magnitude and direction of the applied force is sensitive to exit area orientation. The trends shown here are not limited to the case of the single ramp nozzle. Similar problems will be encountered with any nozzle design that does not maintain the exit area normal to the flow direction. This is true for nearly all vectoring schemes and particularly true for plug type nozzles or designs using louvers at the nozzle exit to turn the flow. This potential problem does not necessarily have a negative effect, however. If properly integrated and accounted for, changes in force magnitude and direction can result in benefits to the system.

The basic problem arises in situations where a proper accounting of the forces is not made, resulting in erroneous conclusions being drawn. Caution is particularly important in the formulation of wind tunnel tests to determine the external installation benefits attributable to non-axisymmetric nozzle types. In such tests and in system studies it is best to treat the gross thrust as a vector quantity whose orientation may be a function of nozzle pressure ratio as well as nozzle deflection angle.



FORCE APPLIED NOT NECESSARILY EQUAL TO $M_0 V_0 + (P_{00} - P_{00}) A_0$

Figure 34. Family of Single Ramp Nozzles

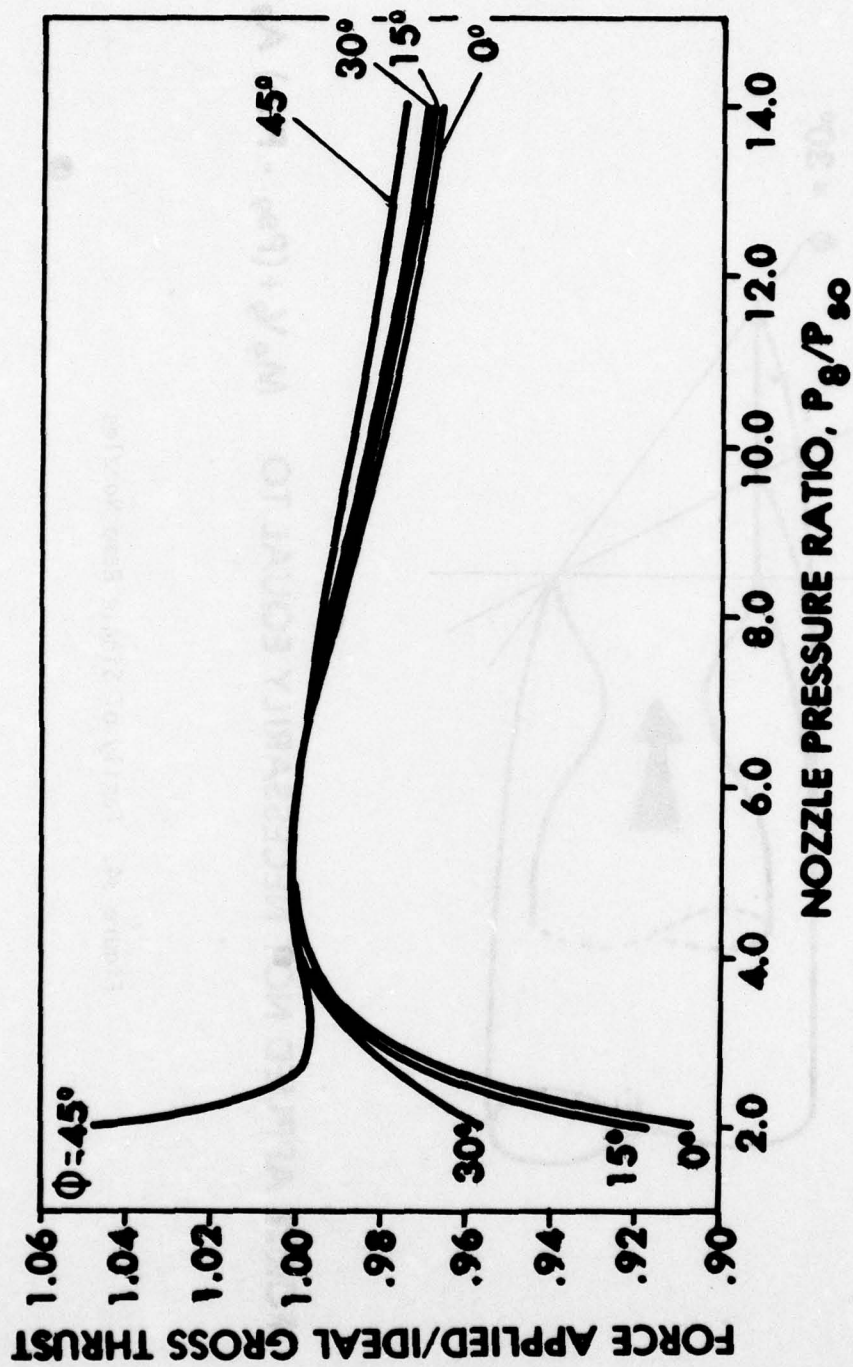


Figure 35. Internal Performance

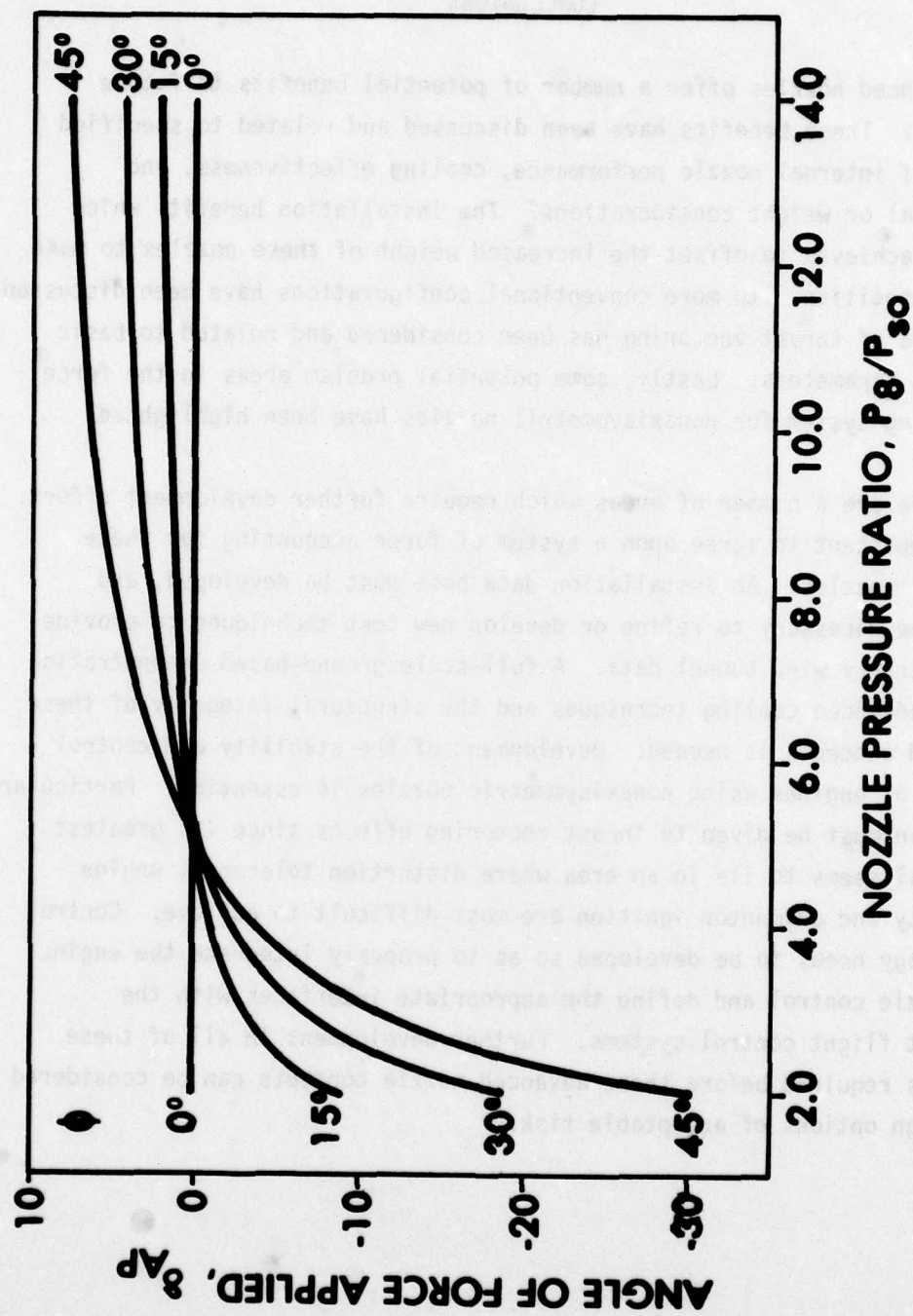


Figure 36. Angle at Which Thrust Is Applied

SECTION VII

CONCLUSIONS

Advanced nozzles offer a number of potential benefits to future aircraft. These benefits have been discussed and related to specified levels of internal nozzle performance, cooling effectiveness, and structural or weight considerations. The installation benefits which must be achieved to offset the increased weight of these nozzles to make them competitive with more conventional configurations have been discussed. The value of thrust vectoring has been considered and related to basic aircraft parameters. Lastly, some potential problem areas in the force accounting system for nonaxisymmetric nozzles have been highlighted.

There are a number of areas which require further development effort. It is important to agree upon a system of force accounting for these types of nozzles. An installation data base must be developed, and it may be necessary to refine or develop new test techniques to provide the necessary wind tunnel data. A full-scale ground-based demonstration of the advanced cooling techniques and the structural integrity of these advanced concepts is needed. Development of the stability and control aspects of engines using nonaxisymmetric nozzles is essential. Particular attention must be given to thrust vectoring effects since its greatest potential seems to lie in an area where distortion tolerance, engine stability and augmentor ignition are most difficult to achieve. Control technology needs to be developed so as to properly integrate the engine and nozzle control and define the appropriate interfaces with the aircraft flight control systems. Further development in all of these areas is required before these advanced nozzle concepts can be considered as design options of acceptable risk.